

Black hole quasinormal modes: hints of quantum gravity?

Emanuele Berti

E-mail: berti@wugrav.wustl.edu

*McDonnell Center for the Space Sciences,
Department of Physics, Washington University,
St. Louis, Missouri 63130, USA*

This is a short review of the quasinormal mode spectrum of Schwarzschild, Reissner-Nordström and Kerr black holes, summarizing results obtained in [1, 2, 3]. The summary includes previously unpublished calculations of i) the eigenvalues of spin-weighted spheroidal harmonics, and ii) quasinormal frequencies of extremal Reissner-Nordström black holes.

I. INTRODUCTION

Black holes are one of the most extreme predictions of Einstein's general relativity. They challenge common sense to such an extent that Einstein himself was reluctant to accept their reality. Despite the initial resistance, nowadays the existence of black holes is widely accepted by the physics community. Observationally, the astronomical evidence for black holes is compelling. Theoretically, a key step to accept the idea that black holes are not just a mathematical solution of the Einstein equations *in vacuo* was the proof of the (linear) stability of the Schwarzschild metric. This proof is based on black hole perturbation theory, as developed in two classic papers by Regge-Wheeler and Zerilli [4, 5]. Their formalism gets rid of the angular dependence of the perturbation variables through a tensorial generalization of the spherical harmonics, thus reducing the solution of the perturbed Einstein equations to the study of a Schrödinger-like wave equation with some potential $V(r)$. Stability can then be established by methods that are familiar from quantum mechanics: perturbations due to an external (eg., electromagnetic or gravitational) field are considered as waves scattering off the corresponding potential [6]. It is worth stressing that the causally disconnected region *inside* the event horizon plays no role whatsoever in this analysis.

The Regge-Wheeler/Zerilli formalism was later extended to encompass charged (Reissner-Nordström) or rotating (Kerr) black hole solutions. For Reissner-Nordström (RN) black holes we have *two* coupled Schrödinger equations, describing the mutual interaction of gravitational and electromagnetic perturbations. For Kerr black holes the problem is highly non-trivial, since the background geometry is not spherical and tensor spherical harmonics cannot be used any more. Nonetheless, Teukolsky was able to separate the angular and radial dependence of the perturbations using a certain class of special functions (the *spin-weighted spheroidal harmonics*; see section V C) - a truly remarkable achievement [7]. A complete discussion of black hole perturbation theory can be found in the monumental monograph by Chandrasekhar [8]. The extension to charged *and* rotating (Kerr-Newman) black holes turned out to be a formidable task: the numerous attempts to separate the corresponding perturbation equations have all failed.

Once we know that a black hole solution *is* indeed stable, the next step is to understand “how much stable” it is. In other words, on which timescale does a black hole radiate away its “hair” after formation? The answer to this question is provided by the black hole's *quasinormal mode spectrum*. After an initial phase depending on the details of the collapse, the black hole starts vibrating into “quasinormal” (exponentially decaying) oscillation modes whose frequencies and decay times depend only on the intrinsic features of the black hole itself, being insensitive to the details of the collapse.

We have seen that for Schwarzschild, RN and Kerr black holes the perturbation problem can be reduced to the study of certain characteristic wave equations. The background spacetime curvature determines the shape of the potential in each wave equation. Quasinormal modes are defined as solutions that satisfy “natural” boundary conditions for classical waves: they are purely outgoing at spatial infinity and purely ingoing at the black hole horizon. In the Fourier domain, this is an eigenvalue problem for the wave's (complex) frequency $\omega = \omega_R + i\omega_I$. The two boundary conditions are satisfied by a discrete set of quasinormal frequencies, $\omega = \{\omega_n\}$, where the integer $n = 0, 1, \dots$ labels the modes, which are normally sorted by increasing values of $|\omega_I|$. Quasinormal frequencies are complex (*quasi*-normal) because outgoing waves at infinity radiate energy (the system is not conservative). The damping time of each oscillation is of course given by $\tau = 1/|\omega_I|$: modes having large values of $|\omega_I|$ damp faster. The quasinormal mode spectrum, unlike ordinary normal mode expansions, is not complete: in general, we cannot express a given perturbation as a superposition of quasinormal modes (see section 4.4 of reference [9] for a discussion). Completeness would be desirable from a mathematical point of view, but in any case quasinormal mode expansions are useful (and routinely used) to describe the final stages of formation of a black hole after collapse. For example, it has been shown that the numerical waveforms obtained from general relativistic simulations of distorted black holes are very well fitted using the fundamental quasinormal mode, with the possible addition of a few overtones [10].

The rest of this short review is devoted to a detailed presentation of the quasinormal mode spectrum of

Schwarzschild, RN and Kerr black holes. The quasinormal spectrum has a complicated structure: as it happens, black hole perturbation theory leads us once again “into a realm of the rococo: splendid, joyful, and immensely ornate” [8]. Such an ornate spectrum can at times be hard to compute, even by the most sophisticated numerical methods.

In particular, for a long time the high-damping limit of the spectrum has been a no-go zone. From a physical point of view, it is clear that slowly-damped quasinormal modes should dominate the response of a black hole to any type of perturbation: this obvious consideration initially reduced the impetus to explore the large- $|\omega_I|$ (high damping) regime. From a technical perspective, most numerical methods to impose the quasinormal mode boundary conditions are based on discriminating outgoing waves from ingoing waves. The exponentially decaying solution is quickly swamped into numerical noise, and this effect is larger for larger values of the damping. As a consequence, all numerical methods are doomed to failure at some critical value of $|\omega_I|$.

More recently, the high-damping region of the quasinormal mode spectrum gained more attention because of a conjectured connection with quantum gravity. York [11] first attempted to relate the (purely classical) quasinormal mode spectrum with quantum properties of black holes, and more specifically Hawking radiation. In 1998 Hod [12] noticed that, as $|\omega_I| \rightarrow \infty$, the numerically computed oscillation frequencies of Schwarzschild black holes tend to a constant asymptotic value $\omega_R^* = T_H \ln 3$, where T_H is the Hawking temperature of the black hole. In the same limit, the (constant) spacing between modes is given by $2\pi T_H$. Assuming that the minimum energy emitted or absorbed by a black hole is $\Delta M = \hbar \omega_R^*$ and using the Bekenstein-Hawking area-entropy relationship, Hod found an equally spaced black hole area spectrum (in agreement with some heuristic arguments by Bekenstein [13]). By virtue of the “ $\ln 3$ ” factor, the resulting spectrum is also consistent with a statistical-mechanical interpretation of black hole entropy. The idea was revived more recently by Dreyer [14], who used a similar argument to fix the Barbero-Immirzi parameter [14] - an undetermined constant of proportionality entering black hole entropy calculations in Loop Quantum Gravity.

The results we show here do *not* seem to support an extension of Hod’s original proposal to charged and rotating black holes. In addition, the original Loop Quantum Gravity calculation of the black hole area spectrum was recently re-examined and shown to be in error by Domagala and Lewandowski [15]. These developments could be used to argue against the relevance of quasinormal modes for Loop Quantum Gravity, or any other theory of quantum gravity for that matter. Some hints to clarify – or kill once and for all – the connection between quasinormal modes and area quantization might come from analogue black holes [16], but in that case the thermodynamical interpretation of horizon area as entropy is not a trivial issue.

Whether or not quasinormal frequencies have something to say about quantum gravity, the recent conjectures stimulated a lot of work to clarify the structure of the high-damping region of the quasinormal mode spectrum. The following sections summarize some of these recent developments. Our aim is *not* to give a complete overview of recent work in this field: that would be an ambitious goal. For example, we do not discuss recent progress on the asymptotic quasinormal spectrum of black holes in non-asymptotically flat spacetimes or higher dimensions (with a few exceptions where appropriate). We only present a personal (and therefore biased) account of some open problems, concentrating on the Kerr-Newman family of black hole solutions. Before turning to a description of the quasinormal mode spectrum, it is useful to mention in passing different numerical methods that have been used in the past for quasinormal mode calculations.

II. NUMERICAL METHODS

The summary we present in this section is only meant to highlight pros and cons of some popular numerical methods to compute quasinormal modes, and ultimately to justify our use of the continued fraction technique in the present context. The list is by no means exhaustive. For a more complete discussion of the merits and drawbacks of each method we refer the reader to section 6.1 of [17].

- 1) *Time-domain evolutions* of the Regge-Wheeler and Zerilli equations were first performed by Vishveshwara [18] and Press [19]: this is actually how quasinormal modes were first discovered. However, finding highly damped modes in this way requires long and stable evolutions. This method is not used any more for quasinormal mode calculations, with some notable exceptions in cases where a Fourier-domain treatment is cumbersome or impossible. Examples include i) the simulation of complicated distributions of matter in a fixed (black hole or stellar) background [20], and ii) time evolutions of the Kerr perturbation equations (see [21] and references therein). The latter are particularly important for the simulation of extreme mass ratio inspirals, one of the target sources for the space-based gravitational wave interferometer LISA. No generalization of the Carter constant is known for off-equatorial, non-circular particle orbits in the Kerr metric, and time evolutions provide a valid alternative to calculations of radiation reaction effects using self-force methods.

- 2) *Direct integrations of the wave equation in the frequency domain* were pioneered by Chandrasekhar and Detweiler [22]. The simplest version of this approach is numerically unstable: the exponentially vanishing solution is very hard to extract from numerical noise in the exponentially growing solution, a problem that plagues especially highly damped modes. Several improvements have been attempted. A notable one was introduced by Nollert and Schmidt, who used a sophisticated Laplace transform definition of the quasinormal frequencies [23]. In this framework, the state of the art is probably the complex integration technique developed by Andersson and coworkers [24]. In any case, direct integrations are quite time consuming. Phase-integral based methods (see below) sometimes involve numerical integrations; they can be competitive with continued fraction methods at moderate dampings, but ultimately fail at very high values of $|\omega_I|$.
- 3) *Inverse potential methods* have been introduced by Mashoon and collaborators [25]. The idea is to approximate the exact potential by some simpler potential (eg. a potential of the Pöschl-Teller form) whose spectrum can be found analytically. These techniques can be a valuable tool in certain situations [26], but in general results obtained from approximating potentials should not be expected to be accurate. For example, Nollert showed that approximating the Regge-Wheeler potential by a series of square wells of decreasing width does not yield the expected quasinormal frequencies as the width of the square wells tends to zero. Analytic approximations can still be useful in certain limits, such as the eikonal approximation (large- l limit) or the high damping limit [27, 28, 29].
- 4) *WKB methods* were originally suggested by Schutz and Will [30] and are based on elementary quantum mechanical arguments. The analogy between the wave equation describing black hole perturbations and the Schrödinger equation can be exploited to use standard WKB expansions. At lowest order, quasinormal frequencies are given by the Bohr-Sommerfeld rule:

$$\int_{r_A}^{r_B} [\omega^2 - V(r)]^{1/2} dr = (n + 1/2)\pi, \quad (1)$$

where r_A and r_B are the two roots (turning points) of $\omega^2 - V(r) = 0$. The WKB expansion can be pushed to higher orders [31, 32], allowing a simple and reasonably accurate determination of the quasinormal frequencies and a transparent physical interpretation of the results. The method can be generalized to deal with RN [33] and even Kerr black holes [34]. In the latter case, unfortunately, the WKB method is not very simple to apply (the Kerr potential in the standard Teukolsky equation is complex in the first place, but it can be made real transforming the equation to a different form) and does not yield very accurate results. The WKB approximation gets better for large values of l , allowing an analytic determination of quasinormal frequencies in the large- l limit, but it was found to fail badly at high values of the damping [35].

- 5) *Phase-integral methods* are a substantial improvement over standard WKB techniques [36, 37, 38]. Their major drawback is related to the fact that they require integrations in the complex plane. The integration contour must be found case by case, and the problem can be quite tricky, depending on the singularity structure of the potential. A variant of the phase-integral method has been used to compute analytically the Schwarzschild and RN quasinormal frequency in the limit $|\omega_I| \rightarrow \infty$ [39]. A similar analytical treatment for the Kerr case is still missing.
- 6) *Continued fractions* were first used by Leaver [40] exploiting once again an analogy with quantum mechanics. Leaver's approach is based on a classical 1934 paper by Jaffé on the electronic spectra of the H^+ ion [41]. The key steps are: a) recognize that the wave equations can be seen as special cases of generalized spheroidal wave equations; b) write appropriate series expansions for the solutions; c) replace the series expansions in the differential equations and derive recursion relations for the expansion coefficients; d) use the recursion relations to study the convergence properties of these series and impose quasinormal mode boundary conditions. The determination of quasinormal frequencies boils down to a numerical solution of continued fraction relations involving the mode frequency and the black hole parameters. The evaluation of continued fractions only involves elementary algebraic operations and the convergence of the method is excellent, even at high damping. In the Schwarzschild case, in particular, the method can be tweaked to allow the determination of modes of order up to $\sim 100,000$ [42]. Gauss-Jordan elimination techniques can be used to encompass the RN [43] and even extreme RN [44] cases.

Other approaches may be preferred in specific situations, but Leaver's continued fraction technique is the best workhorse method to compute highly damped modes in general situations. It is very reliable, largely independent of the form of the potential (that is only used to find the recursion coefficients once and for all) and fast, bypassing numerical integrations of the wave equations.

All the results we present in the following have been obtained using different variants of Leaver's method. We adopt geometrical units and consistently use Leaver's conventions [40]; in particular, we set $2M = 1$. This means that extremal Kerr and RN black holes correspond, respectively, to $a = 1/2$ and $Q = 1/2$.

III. SCHWARZSCHILD BLACK HOLES

A. Computational method

Let us begin from the simplest case of spherically symmetric, uncharged, non-rotating Schwarzschild black holes. A detailed derivation of the perturbation equations can be found in [8] (for more details on the computational procedure see [40, 42]). In brief: the angular dependence of the metric perturbations can be separated using tensorial spherical harmonics [5]. Depending on their behavior under parity, the perturbation variables are classified as *polar* (even) or *axial* (odd). We can get rid of the time dependence using a standard Fourier decomposition for each perturbation variable ψ :

$$\psi(t, r) = \frac{1}{2\pi} \int_{-\infty}^{+\infty} e^{-i\omega t} \psi(\omega, r) d\omega. \quad (2)$$

The resulting differential equations can be manipulated to yield two wave equations, one for the polar perturbations (that we shall denote by a superscript plus) and one for the axial perturbations (superscript minus):

$$\left(\frac{d^2}{dr_*^2} + \omega^2 \right) Z^\pm = V^\pm Z^\pm, \quad (3)$$

where we introduced a tortoise coordinate r_* defined in the usual way by the relation

$$\frac{dr}{dr_*} = \frac{\Delta}{r^2}, \quad (4)$$

and $\Delta = r(r - 1)$.

Polar perturbations are related to axial perturbations by a differential transformation discovered by Chandrasekhar [8]. As anticipated in the introduction, quasinormal modes are solutions of equation (3) that are purely outgoing at spatial infinity ($r \rightarrow \infty$) and purely ingoing at the black hole horizon ($r \rightarrow 1$). These boundary conditions are only satisfied by a discrete set of complex frequencies (the quasinormal frequencies). For the Schwarzschild solution the two potentials V^\pm are quite different, yet the quasinormal modes for polar and axial perturbations are the same [8]. This can be seen as a consequence of the two potentials being related by a supersymmetry transformation [45]. Since polar and axial perturbations are isospectral and V^- has an analytic expression which is simpler to handle, we can concentrate on the axial equation. Written in terms of the “standard” radial variable r , this equation reads:

$$r(r-1) \frac{d^2 \psi_l}{dr^2} + \frac{d\psi_l}{dr} - \left[l(l+1) - \frac{s^2-1}{r} - \frac{\omega^2 r^3}{r-1} \right] \psi_l = 0, \quad (5)$$

where s is the spin weight of the perturbing field ($s = 0, -1, -2$ for scalar, electromagnetic and gravitational perturbations, respectively) and l is the angular index of the perturbation. Notice that perturbations of a Schwarzschild background are independent of the azimuthal quantum number m , because the background spacetime has spherical symmetry; the same is true in the RN case, but not for Kerr black holes. Equation (5) can be solved using a series expansion of the form:

$$\psi_l = (r-1)^{-i\omega} r^{2i\omega} e^{i\omega(r-1)} \sum_{j=0}^{\infty} a_j \left(\frac{r-1}{r} \right)^j. \quad (6)$$

where the prefactor is chosen to incorporate the quasinormal boundary conditions at the two boundaries. Substituting the series expansion (6) in (5) we get a three term recursion relation for the expansion coefficients a_j :

$$\begin{aligned} \alpha_0 a_1 + \beta_0 a_0 &= 0, \\ \alpha_j a_{j+1} + \beta_j a_j + \gamma_j a_{j-1} &= 0, \quad j = 1, 2, \dots \end{aligned} \quad (7)$$

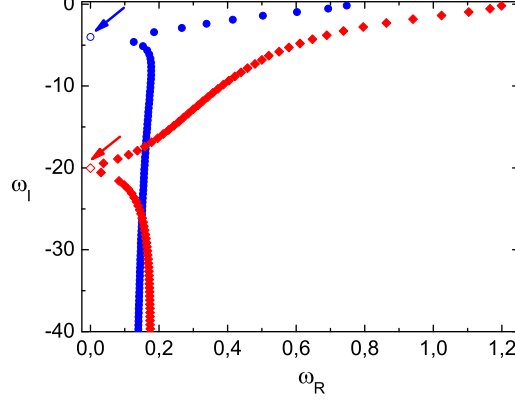


FIG. 1: Quasinormal frequencies for gravitational perturbations with $l = 2$ (blue circles) and $l = 3$ (red diamonds). Compare eg. Figure 1 in [42]. In both cases we mark by an arrow the algebraically special mode, that is given analytically by Equation (13); a more extensive discussion of this mode is given in section VI. Notice that as the imaginary part of the frequency tends to infinity the real part tends to a finite, l -independent limit.

where α_j , β_j and γ_j are simple functions of the frequency ω , l and s . Their explicit form can be found in [40]. The quasinormal mode boundary conditions are satisfied when the following continued-fraction condition on the recursion coefficients holds:

$$0 = \beta_0 - \frac{\alpha_0 \gamma_1}{\beta_1 - \frac{\alpha_1 \gamma_2}{\beta_2 - \dots}} \quad (8)$$

The n -th quasinormal frequency is (numerically) the most stable root of the n -th inversion of the continued-fraction relation (8), i.e., it is the root of

$$\beta_n - \frac{\alpha_{n-1} \gamma_n}{\beta_{n-1} - \frac{\alpha_{n-2} \gamma_{n-1}}{\beta_{n-2} - \dots}} \dots \frac{\alpha_0 \gamma_1}{\beta_0} = \frac{\alpha_n \gamma_{n+1}}{\beta_{n+1} - \frac{\alpha_{n+1} \gamma_{n+2}}{\beta_{n+2} - \dots}} \dots \quad (n = 1, 2, \dots). \quad (9)$$

The infinite continued fraction appearing in equation (9) can be summed “bottom to top” starting from some large truncation index N . Nollert [42] has shown that the convergence of the procedure improves if the sum is started using a wise choice for the value of the “rest” of the continued fraction, R_N , defined by the relation

$$R_N = \frac{\gamma_{N+1}}{\beta_{N+1} - \alpha_{N+1} R_{N+1}}. \quad (10)$$

Assuming that the rest can be expanded in a series of the form

$$R_N = \sum_{k=0}^{\infty} C_k N^{-k/2}, \quad (11)$$

it turns out that the first few coefficients in the series are $C_0 = -1$, $C_1 = \pm \sqrt{-2i\omega}$, $C_2 = (3/4 + 2i\omega)$ and $C_3 = [l(l+1)/2 + 2\omega^2 + 3i\omega/2 + 3/32]/C_1$ (the latter coefficient contains a typo in [42], but it is numerically irrelevant anyway).

B. Results

We computed quasinormal frequencies using Leaver’s technique as improved by Nollert. The slowly damped modes of the resulting spectrum for $l = 2$ and $l = 3$ are shown in Table I and Figure 1. Reintroducing physical units, the fundamental oscillation frequency $f = \omega_R/(2\pi)$ and the damping time $\tau = 1/|\omega_I|$ of an astrophysical black hole scale with mass according to the relation

$$f = 1.207 \left(\frac{10 M_\odot}{M} \right) \text{ kHz}, \quad \tau = 0.5537 \left(\frac{M}{10 M_\odot} \right) \text{ ms}. \quad (12)$$

TABLE I: Representative Schwarzschild quasinormal frequencies for $l = 2$ and $l = 3$ (from [40]).

	$l = 2$	$l = 3$
n	ω_n	ω_n
1	(0.747343,-0.177925)	(1.198887,-0.185406)
2	(0.693422,-0.547830)	(1.165288,-0.562596)
3	(0.602107,-0.956554)	(1.103370,-0.958186)
4	(0.503010,-1.410296)	(1.023924,-1.380674)
5	(0.415029,-1.893690)	(0.940348,-1.831299)
6	(0.338599,-2.391216)	(0.862773,-2.304303)
7	(0.266505,-2.895822)	(0.795319,-2.791824)
8	(0.185617,-3.407676)	(0.737985,-3.287689)
9	(0.000000,-3.998000)	(0.689237,-3.788066)
10	(0.126527,-4.605289)	(0.647366,-4.290798)
11	(0.153107,-5.121653)	(0.610922,-4.794709)
12	(0.165196,-5.630885)	(0.578768,-5.299159)
20	(0.175608,-9.660879)	(0.404157,-9.333121)
30	(0.165814,-14.677118)	(0.257431,-14.363580)
40	(0.156368,-19.684873)	(0.075298,-19.415545)
41	(0.154912,-20.188298)	(-0.000259,-20.015653)
42	(0.156392,-20.685630)	(0.017662,-20.566075)
50	(0.151216,-24.693716)	(0.134153,-24.119329)
60	(0.148484,-29.696417)	(0.163614,-29.135345)

An “algebraically special” mode, whose frequency is (almost) pure imaginary, separates the lower quasinormal mode branch from the upper branch [46]. This algebraically special mode has a very peculiar nature, as we will see in section VI. It is located at

$$\tilde{\Omega}_l = \pm i \frac{(l-1)l(l+1)(l+2)}{6}, \quad (13)$$

and it can be taken as roughly marking the onset of the asymptotic high-damping regime. The algebraically special mode quickly moves downwards in the complex plane as l increases: from Table I we see that it corresponds to an overtone index $n = 9$ when $l = 2$, and to an overtone index $n = 41$ when $l = 3$. This means that for high values of l the asymptotic high-damping regime sets in later, becoming harder to probe using numerical methods.

Nollert was able to compute for the first time highly damped quasinormal frequencies corresponding to *gravitational* perturbations [42]. His main result was that the real parts of the quasinormal frequencies are well fitted, for large n , by a relation of the form

$$\omega_R = \omega_\infty + \frac{\lambda_{s,l}}{\sqrt{n}}. \quad (14)$$

The leading-order fitting coefficient $\omega_\infty = 0.0874247$ is independent of l . Corrections of order $\sim n^{-1/2}$, however, are l -dependent (we will see in a moment that they also depend on the spin s of the perturbing field; that’s why we denoted them by $\lambda_{s,l}$). For gravitational perturbations ($s = -2$) Nollert found that $\lambda_{-2,2} = 0.4850$, $\lambda_{-2,3} = 1.067$, $\lambda_{-2,6} = 3.97$. Numerical data for scalar perturbations ($s = 0$) are also well fitted by formula (14), and the asymptotic frequency for scalar modes is exactly the same. Only the leading-order correction coefficients $\lambda_{0,l}$ are different: $\lambda_{0,0} = 0.0970$, $\lambda_{0,1} = 0.679$, $\lambda_{0,2} = 1.85$ [1].

These numerical results are perfectly consistent with analytical calculations. Motl [27] analyzed the continued fraction condition (8) to find that highly damped quasinormal frequencies satisfy the relation

$$\omega \sim T_H \ln 3 + (2n+1)\pi i T_H + \mathcal{O}(n^{-1/2}). \quad (15)$$

(remember that in our units $2M = 1$, so that the Hawking temperature of a Schwarzschild black hole $T_H = 1/4\pi$). This conclusion was later confirmed by complex-integration techniques [28] and phase-integral methods [39]. Neitzke [29]

first suggested that leading order corrections to the asymptotic frequency should be proportional to $[(s^2 - 1) - 3l(l+1)]$; this is consistent with the numerical values of the $\lambda_{s,l}$'s. The proportionality constant is dependent on s : $\lambda_{s,l} = k_s[(s^2 - 1) - 3l(l+1)]$. Maassen van den Brink [79] derived k_{-2} analytically, finding

$$k_{-2} = -\frac{\sqrt{2}[\Gamma(1/4)]^4}{432\pi^{5/2}} \simeq -0.0323356, \quad (16)$$

in perfect agreement with the numerical data, that yield $k_{-2} = -0.0323$, $k_0 = -0.0970 = 3k_{-2}$ [1].

Finally, a systematic perturbative approach to determine lower-order corrections to formula (14) has been developed in [47]. Their final result, valid for scalar and gravitational perturbations, is again perfectly consistent with numerical data. The perturbative technique used in [47] has also been extended to higher-dimensional Schwarzschild-Tangherlini black holes with the result [48]

$$\omega = T_H \ln(1 + 2 \cos \pi j) + (2n + 1)\pi i T_H + k_D \omega_I^{-(D-3)/(D-2)}, \quad (17)$$

where the coefficient k_D can be determined analytically for given values of D and j [49].

Leaver's method can easily be generalized to these higher-dimensional black holes [48]; the recursion relation has four terms for vector-gravitational and tensor-gravitational perturbations (see also [50] for similar calculations using WKB methods). The most impressive example of an application of Leaver's technique to date is probably reference [51]. There the continued fraction method has been used for a detailed calculation of scalar-gravitational quasinormal frequencies in the case of 5-dimensional Schwarzschild black holes using an *eight-term* recursion relation.

In conclusion, all numerical and analytical results for non-rotating black holes are in perfect agreement. As $|\omega_I| \rightarrow \infty$ scalar and gravitational oscillation frequencies of non-rotating Schwarzschild-Tangherlini black holes *in all dimensions* tend to the constant value $\omega_R = T_H \ln 3$ (this was first argued in [28] and explicitly shown in [52]). For electromagnetic perturbations the situation is less clear: analytical and numerical results in $D = 4$ suggest that the asymptotic limit should be $\omega_R = 0$. For electromagnetic perturbations in $D = 5$, formula (17) doesn't even make sense: this probably means that there are no asymptotic quasinormal frequencies at all (a possibility first suggested in [28]). A similar behavior occurs for the 3-dimensional "draining bathtub" metric describing a rotating acoustic black hole [16], suggesting that this feature may somehow be related to odd-dimensional spacetimes.

IV. REISSNER-NORDSTRÖM BLACK HOLES

A. Computational method

The computational procedure described in the previous section can be generalized to RN black holes. Here we only sketch the key steps, referring the reader to [43] for more details. As usual we define a tortoise coordinate r_* by the relation (4), but now $\Delta = r^2 - r + Q^2$ (recall that in our units $0 \leq Q \leq 1/2$). Explicitly, the tortoise coordinate can be written as

$$r_* = r + \frac{r_+^2}{r_+ - r_-} \ln(r - r_+) - \frac{r_-^2}{r_+ - r_-} \ln(r - r_-), \quad (18)$$

where $r_{\pm} = (1 \pm \sqrt{1 - 4Q^2})/2$ is the location of the inner (Cauchy) and outer (event) horizons of the RN metric. After separation of the angular dependence and Fourier decomposition, electromagnetic and axial-gravitational perturbations of the RN metric are described by two wave equations,

$$\left(\frac{d^2}{dr_*^2} + \omega^2 \right) Z_i^- = V_i^- Z_i^-, \quad (19)$$

where

$$V_i^- = \frac{\Delta}{r^5} \left[l(l+1)r - q_j + \frac{4Q^2}{r} \right], \quad i, j = 1, 2 \ (i \neq j), \quad (20)$$

and

$$q_1 = \left[3 + \sqrt{9 + 16Q^2(l-1)(l+2)} \right] / 2, \quad q_2 = \left[3 - \sqrt{9 + 16Q^2(l-1)(l+2)} \right] / 2. \quad (21)$$

As in the Schwarzschild case, the polar perturbation variables (Z_i^+) can be obtained from the axial variables (Z_i^-) by a Chandrasekhar transformation [8], so we do not consider them in the following. In the limit $Q \rightarrow 0$ the potentials

V_1^- and V_2^- describe, respectively, purely electromagnetic [spin weight $s = -1$ in Equation (5)] and pure axial-gravitational [spin weight $s = -2$ in Equation (5)] perturbations of a Schwarzschild black hole; but for any non-zero value of the charge, electromagnetic and gravitational perturbations are tangled. The perturbation equations are solved by a series expansion of the form

$$Z_i^- = \frac{r_+ e^{-2i\omega r_+} (r_+ - r_-)^{-2i\omega - 1} (r - r_-)^{1+i\omega} e^{i\omega r}}{r} u^{-i\omega r_+^2/(r_+ - r_-)} \sum_{j=0}^{\infty} a_j u^j, \quad (22)$$

where $u = (r - r_+)/ (r - r_-)$. The coefficients a_j of the expansion are now determined by a four-term recursion relation whose coefficients depend on the angular index l , on the frequency ω and on the charge Q . The problem can be reduced to a three-term recursion relation of the form (8) using a Gaussian elimination step (see [43] for details). Then we can use again a continued-fraction condition to determine quasinormal frequencies, and Nollert's procedure can be applied to accelerate convergence for large values of the damping. The first few coefficients in the series (11) are now $C_0 = -1$, $C_1 = \pm \sqrt{-2i\omega(2r_+ - 1)}$, $C_2 = (3/4 + 2i\omega r_+)$.

Due to convergence reasons, continued fraction calculations become more and more computationally intensive for large values of the charge [43]. In the limit of maximally charged black holes ($Q = 1/2$) the wave equations have a different singularity structure, and deserve a special treatment [44]. We discuss the peculiarities of the extremal RN case in section IV C.

B. Results

The first few overtones of a RN black hole were studied numerically by Andersson and Onozawa [37, 53] using different numerical methods [54]. These studies revealed a very peculiar behavior.

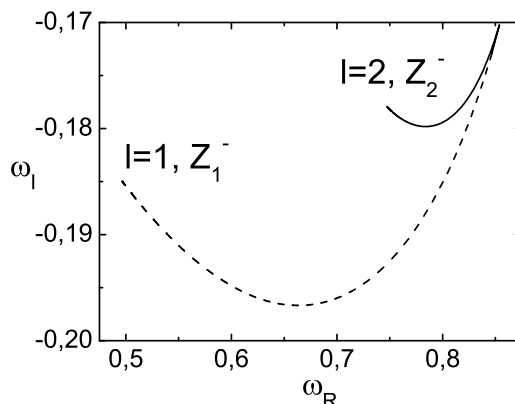


FIG. 2: Trajectory described in the complex-frequency plane by the fundamental RN quasinormal mode as the charge is increased. The solid line corresponds to $l = 2$ and Z_2^- (perturbations that reduce to the axial-gravitational Schwarzschild case as $Q \rightarrow 0$); the dashed line, to $l = 1$ and Z_1^- (purely electromagnetic Schwarzschild perturbations in the limit $Q \rightarrow 0$). The modes coalesce in the extremal limit $Q \rightarrow 1/2$.

The solid line in Figure 2 is the trajectory described in the complex-frequency plane by the fundamental quasinormal mode with $l = 2$ corresponding to Z_2^- (perturbations that reduce to the axial-gravitational Schwarzschild case). The dashed line is the same trajectory for the fundamental quasinormal mode with $l = 1$ corresponding to Z_1^- (which limits us to purely electromagnetic perturbations). The Schwarzschild limit corresponds to the bottom left of each curve, and the trajectories are described counterclockwise as Q increases. The real part of the frequency grows monotonically with Q , and the imaginary part shows a relative minimum. This behavior can easily be understood using WKB arguments: restoring the mass in the equations, the lowest order WKB approximation yields

$$\omega_R \sim \left(l + \frac{1}{2}\right) \sqrt{\frac{(M - Q^2/r_0)}{r_0^3}}, \quad \omega_I \sim -\frac{1}{2} \sqrt{\frac{(M - Q^2/r_0)(3M - 4Q^2/r_0)}{r_0^4}}, \quad (23)$$

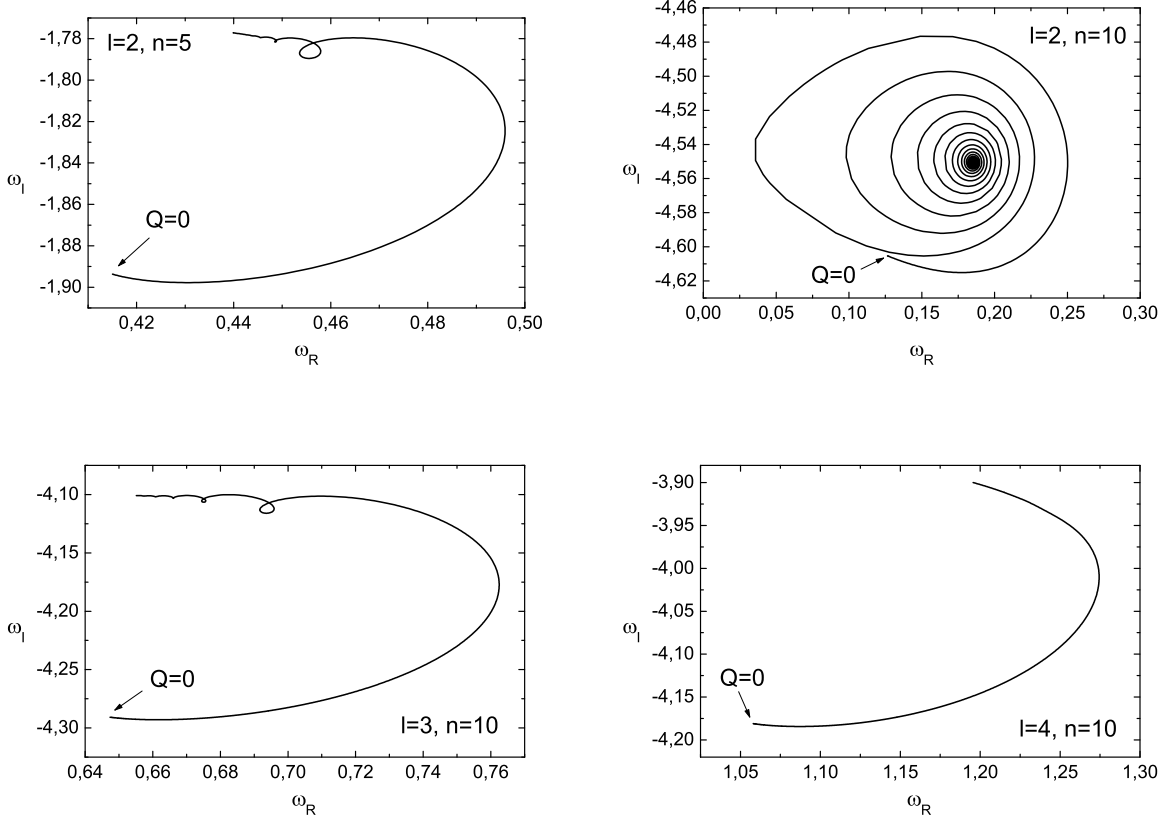


FIG. 3: The top two panels show the behavior of the $n = 5$ and $n = 10$ quasinormal frequencies in the complex ω plane. The $n = 10$ mode “spirals in” towards its value in the extremal charge limit; the number of spirals described by each mode increases roughly as the mode order n . The panels in the second row show how the $n = 10$ spiral “unwinds” as the angular index l is increased (in other words, the asymptotic behavior sets in later for larger l ’s). In all cases, we have marked by an arrow the frequency corresponding to the Schwarzschild limit ($Q = 0$).

where $r_0 \sim (3M + \sqrt{9M^2 - 8Q^2})/2$ is the location of the potential peak. It is worth noting that *modes of Z_2^- with angular index l coalesce with modes of Z_1^- with index $(l - 1)$ in the extremal limit*. This is a general feature we are going to discuss in section IV C.

The algebraically special frequency of Reissner-Nordström black holes can be found using the same reasoning as in the Schwarzschild case [46]. It reads

$$\tilde{\Omega}_l^{(i)} = \pm i \frac{(l-1)l(l+1)(l+2)}{3 \left[1 \pm \sqrt{1 + 4Q^2(l-1)(l+2)} \right]}, \quad (24)$$

where the superscript (i) refers to the two different potentials in Equation (19). For extremal black holes ($Q = 1/2$) the first algebraically special mode for $l = 2$ is located at $\Omega = -3i$.

In the rest of this section we explore the high-damping regime. We fix our attention on the wave equation for Z_2^- (perturbations reducing to gravitational perturbations of Schwarzschild as $Q \rightarrow 0$); results for Z_1^- are similar. As can be seen in Figures 3, 4 and 5, the behavior of high order modes is quite surprising. At first the trajectories described by the modes in the complex- ω plane show closed loops, as in the top left panel of Figure 3. Then they get a spiral-like shape, moving out of their Schwarzschild value and looping in towards some limiting frequency as Q tends to the extremal value. This kind of behavior is shown in the top right panel of Figure 3. We observe that such a spiralling behavior sets in for larger values of the modes’ imaginary part (i.e., larger values of n) as the angular index l increases. In other words, increasing l for a given value of the mode index n has the effect of unwinding the spirals. This can be seen in the two bottom panels of Figure 3. However, for each l the spiralling behavior is eventually observed when n is large enough.

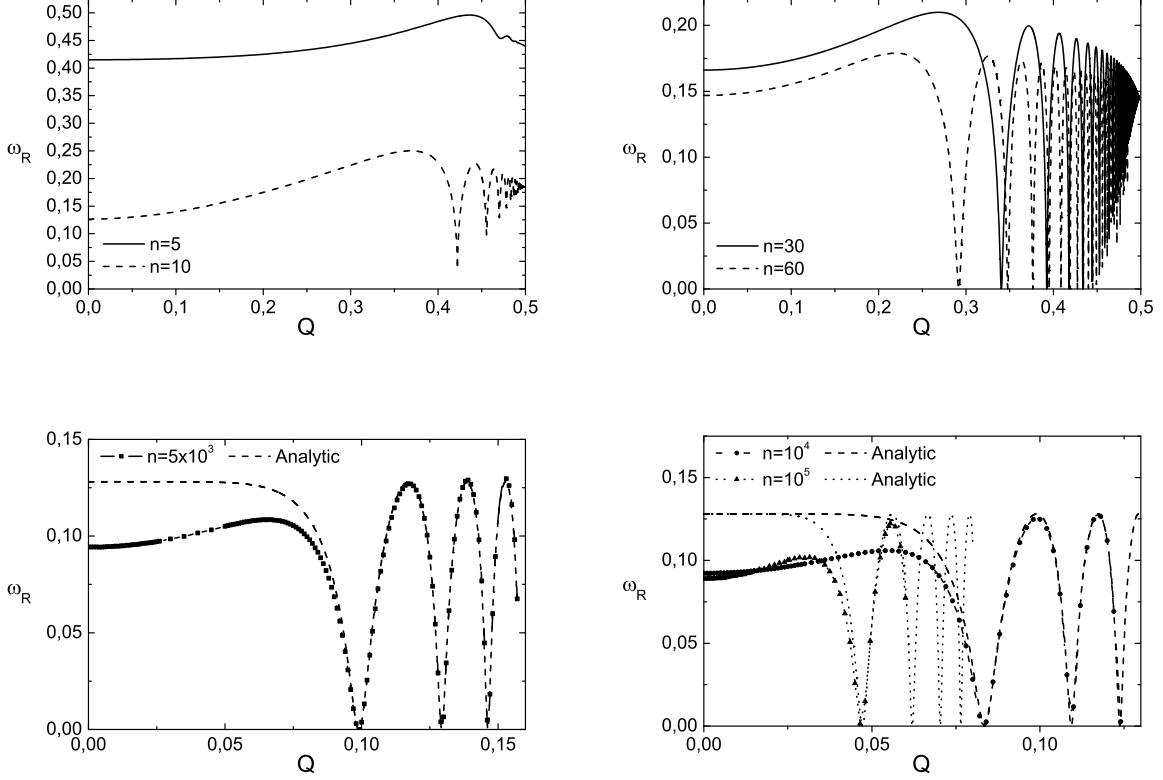


FIG. 4: Real part of the RN quasinormal frequencies as a function of charge for $n = 5, 10, 30, 60, 5000, 10000, 100000$. As the mode order increases the computation becomes more and more time consuming, the oscillations become faster, and a good numerical sampling is rather difficult to achieve; therefore in the last plot we use different symbols (small squares, circles and triangles) to display the actually computed points. For $n = 5000, 10000, 100000$ we also compare to the prediction of the analytic formula (25) derived by Motl and Neitzke [28]. The oscillatory behavior is reproduced extremely well by their formula, but the disagreement increases for small charge: formula (25) does not yield $T_H \ln 3$ in the Schwarzschild limit.

A perhaps clearer picture of the modes' behavior can be obtained looking separately at the real and imaginary parts of the mode frequencies as function of modes. Let us focus first on the real parts. The corresponding numerical results are shown in Figure 4. It is quite apparent that, as the mode order grows, the oscillating behavior as a function of charge start earlier and earlier. For large n the oscillations become faster, the convergence of the continued fraction method slower, and the required computing time gets longer. Therefore, when the imaginary part increases it becomes more difficult to follow the roots numerically as we approach the extremal value $Q = 1/2$. That's why data for very large values of n do not cover the whole range of allowed values for Q . Despite these difficulties, we have many reasons to trust our numerics. We have carefully checked our results, using first double and then quadrupole precision in our Fortran codes (indeed, as n increases, we can obtain results for large values of the charge only using quadrupole precision). Our frequencies accurately reproduce Nollert's results in the Schwarzschild limit, so the numerics can be trusted for small values of Q . More importantly, at large values of the charge numerical data are in excellent agreement with analytical predictions [28]. Motl and Neitzke found the following result for the asymptotic frequencies of scalar and electromagnetic-gravitational perturbations of a RN black hole [55]:

$$e^{\beta\omega} + 2 + 3e^{-\beta_I\omega} = 0. \quad (25)$$

This implicit formula for the asymptotic quasinormal modes was later rederived by an indepent method in [39]. The complex solutions of Equation (25) exactly overlap with the oscillations we observe at large damping for large enough values of Q (see Figures 4 and 5). This agreement gives support to the asymptotic formula (25) and confirms that the numerical calculation is still accurate for large values of Q [29].

Similar considerations apply to the imaginary parts. Some plots illustrating the general trend are shown in Figure

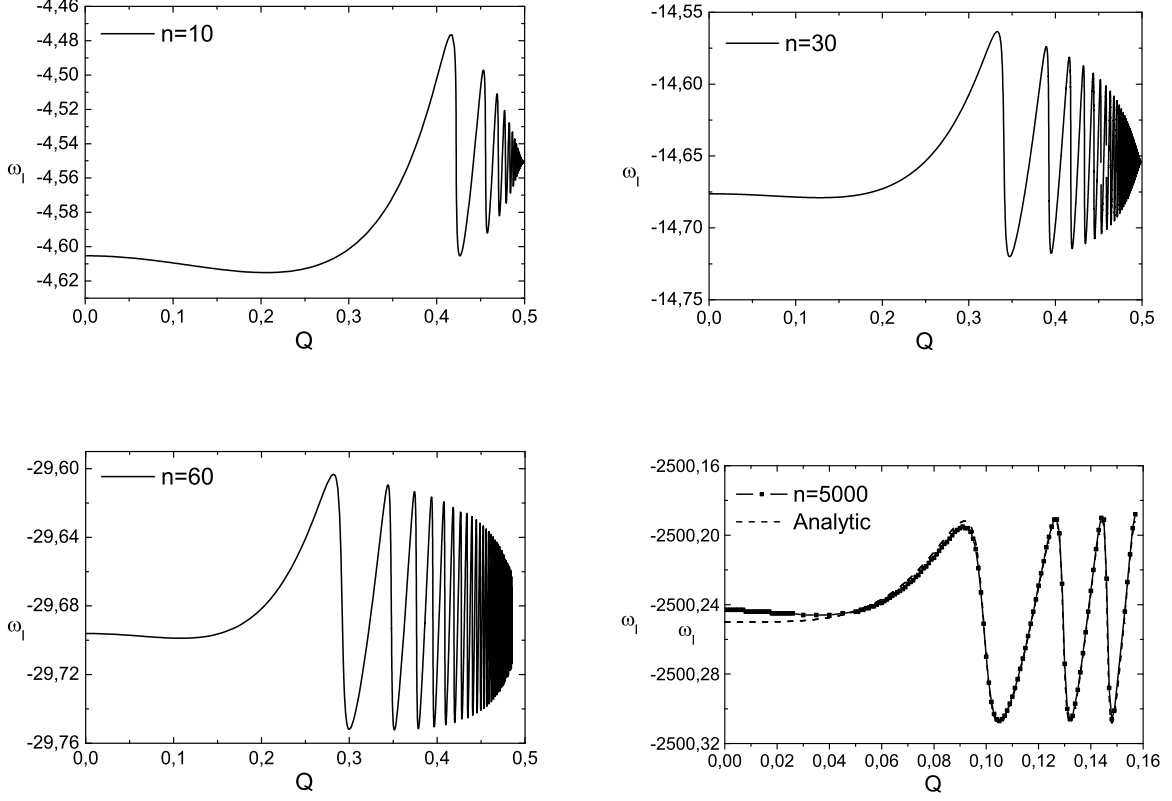


FIG. 5: Imaginary part of the RN quasinormal frequencies as a function of charge for $n = 10, 30, 60, 5000$. For $n = 5000$ we also display the actually computed points, and compare to the prediction of the analytic formula (25). As for the real part, the oscillations are reproduced extremely well, but the disagreement with our numerical data increases for small charge.

5. Once again the numerics show excellent agreement with the asymptotic formula (25) as n increases. The analytic formula deviates from numerical results only for small values of the charge.

In conclusion, numerical results lend strong support to the analytical expression (25). This formula presents us with some striking puzzles. As emphasized in [28, 29], the predicted asymptotic RN quasinormal frequencies do not reduce to the expected Schwarzschild limit, Equation (15). One finds instead

$$\omega_R \rightarrow T_H \ln 5 \quad \text{as} \quad Q \rightarrow 0, \quad (26)$$

a prediction that is hard to reconcile with Hod's interpretation of the asymptotic quasinormal spectrum. Surprisingly, in the extremal limit $Q \rightarrow 1/2$ the real part of the frequency predicted by Equation (25) coincides with the Schwarzschild value:

$$\omega_R \rightarrow T_H \ln 3 \quad \text{as} \quad Q \rightarrow 1/2. \quad (27)$$

It is not clear to which extent this result is relevant: in the extremal limit the two horizons coalesce, the topology of the singularities in the differential equation changes, and the problem may require a separate analysis. Indeed, there are some arguments that the asymptotic oscillation frequency for extremal RN black holes is *not* given by Equation (27) [56].

Another bizarre prediction is that – according to Equation (25) – asymptotic quasinormal frequencies of charged black holes depend not only on the black hole's Hawking temperature, but also on the Hawking temperature of the (causally disconnected) inner horizon. The dependence on the causally disconnected region is not surprising when one looks at the calculation by Motl and Neitzke: their result depends only on the behavior of the potential close to the curvature singularity. Still, the region inside the event horizon plays no role whatsoever in the classical analysis of black hole perturbations. From this perspective, the appearance of β_I in Equation (25) is somehow disturbing.

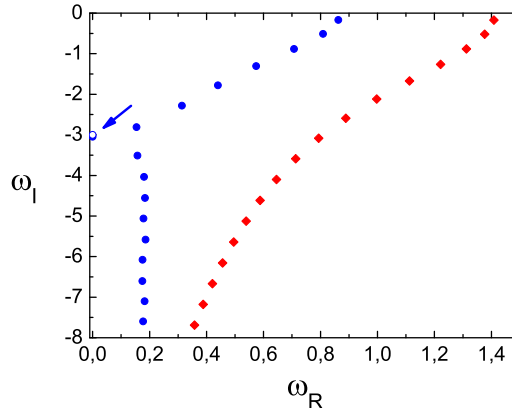


FIG. 6: Quasinormal frequencies for gravitational-type perturbations of an extremal RN black hole with $l = 2$ (blue circles) and $l = 3$ (red diamonds). The spectrum for electromagnetic-type perturbations with $l = 1$ and $l = 2$ would be exactly the same. We mark by an arrow the location of the algebraically special mode. We find a quasinormal mode at $\omega = (0, -3.047876)$ [filled blue circle], while Chandrasekhar’s formula (24) predicts a mode at $\omega = (0, -3)$ [empty blue circle]. Unfortunately the numerical method becomes unstable for values of $|\omega_I| \gtrsim 10$, and cannot be used to verify the prediction (27) of the Motl-Neitzke formula (25).

An interesting classification of the solutions of Equation (25) can be found in Figure 3 and section 4.4 of [39]. Besides “spiralling” solutions the equation also admits *periodic* solutions when $\kappa \equiv \sqrt{1 - Q^2/M^2}$ is a rational number, and even *pure imaginary* solutions that may not be quasinormal modes at all!

To conclude this section: analytical and numerical calculations indicate that (25) is correct. Still, we are far from a full understanding of the physical meaning of this equation and its relation with the asymptotic Schwarzschild quasinormal spectrum (15).

C. Extremal Reissner-Nordström black holes

Leaver’s method fails in the extremal limit. In this limit the two horizons coalesce ($r_{\text{hor}} = r_+ = r_- = 1/2$). The tortoise coordinate becomes, in our units,

$$r_* = r + \ln(2r - 1) - \frac{1}{4r - 2}, \quad (28)$$

and the radial wave equation has irregular singular points at the horizon and at infinity. The series expansion (22) is not valid any more. The trick used by Onozawa *et al.* [44] is to change the expansion variable: they expand in $u = (r - 2r_{\text{hor}})/r$. This choice pushes the horizon to $u = -1$ and infinity to $u = 1$. The requirement that a series solution of the form $\sum_j a_j u^j$ converges at both boundaries means that $\sum_j a_j$ and $\sum_j (-1)^j a_j$ should both be finite; that is, that both $\sum_j a_{2j}$ and $\sum_j a_{2j+1}$ must be convergent. Substitution of the series $\sum_j a_j u^j$ in the differential equation yields a five-term recurrence relation. This five-term recurrence relation can be split in *two* separate five-term recurrence relations, corresponding to the convergence conditions for even and odd coefficients. Finally, the even and odd five-term recurrence relations are reduced to three terms by two iterations of a Gaussian elimination step.

A careful analysis of the extremal RN case is interesting for many reasons. First of all, as we have anticipated (see Figure 2), the quasinormal mode spectrum for extremal RN black holes is characterized by an isospectrality between electromagnetic and gravitational perturbations: *modes of Z_2^- with angular index l coalesce with modes of Z_1^- with index $(l - 1)$ in the extremal limit.* This has been shown to be a manifestation of supersymmetry [57]. The supersymmetric nature of extremal Reissner-Nordström black holes is an attractive feature for the calculation of quantum effects, and it has been exploited in various contexts. Furthermore, topological arguments have been used to show that the entropy-area relation breaks down for extremal RN black holes [58]. So we believe that some caution is required in claiming that the connection between quasinormal modes and the area spectrum is still valid for extreme black holes, as recently advocated in [59]. These problems may be connected with the finding that extremally charged black holes in a (non-asymptotically flat) anti-de Sitter spacetime could in principle be marginally unstable [60].

The explicit analysis of the extremal RN case confirms the above picture [44]. It also shows that the standard Leaver method is surprisingly accurate even in this “extreme” situation, where it is not supposed to converge at all! Indeed, the largest error on the real frequency of the fundamental gravitational mode introduced by the “naive” Leaver treatment is only $\sim 3\%$. The authors of [44] derived only a handful of quasinormal frequencies (namely the first three overtones for different values of l). As far as we know, results for extremal RN black holes in the intermediate damping regime have never been published to date. We show the resulting quasinormal spectrum in Figure 6 (to be compared with Figure 1).

Extremal RN quasinormal frequencies have a similar pattern to Schwarzschild frequencies. Their real part first decreases, approaching the pure-imaginary axis as the overtone index grows. We find a quasinormal mode at $\omega = (0, -3.047876)$, while Chandrasekhar’s formula (24) predicts a mode at $\omega = (0, -3)$. Then ω_R increases again, apparently approaching a constant value that could be compatible with the prediction (27) of the Motl-Neitzke asymptotic formula (25). Unfortunately it is hard to get stable numerical results for values of $|\omega_I| \gtrsim 10$ to explicitly verify this prediction. This relative numerical instability is not unexpected, since a) we need to solve simultaneously two different continued fraction relations, and b) for each of them we must carry out two Gaussian elimination steps.

V. KERR BLACK HOLES

A. Computational method

As in the RN case, here we only give the basic steps of our computational procedure. More details can be found in [40, 42, 61]. For Kerr black holes, the perturbation problem can be reduced to two ordinary differential equations for the angular and radial parts of the perturbations, respectively. In Boyer-Lindquist coordinates, defining $u = \cos\theta$, the angular equation reads

$$[(1-u^2)S_{lm,u}]_{,u} + \left[(a\omega u)^2 - 2a\omega s u + s + {}_s A_{lm} - \frac{(m+su)^2}{1-u^2} \right] S_{lm} = 0, \quad (29)$$

and the radial one

$$\Delta R_{lm,rr} + (s+1)(2r-1)R_{lm,r} + V(r)R_{lm} = 0, \quad (30)$$

where

$$V(r) = \{ [(r^2 + a^2)^2 \omega^2 - 2am\omega r + a^2 m^2 + is(am(2r-1) - \omega(r^2 - a^2))] \Delta^{-1} + [2is\omega r - a^2 \omega^2 - {}_s A_{lm}] \}. \quad (31)$$

The parameter $s = 0, -1, -2$ for scalar, electromagnetic and gravitational perturbations respectively, a is the Kerr rotation parameter ($0 \leq a \leq 1/2$), and ${}_s A_{lm} = {}_s A_{lm}(a\omega)$ is an angular separation constant. In the Schwarzschild limit $a = 0$ the angular separation constant can be determined analytically, and is given by the relation ${}_s A_{lm} = l(l+1) - s(s+1)$.

Boundary conditions for the angular and radial equations yield *two* three-term continued fraction relations of the form (8). Finding quasinormal frequencies is a two-step procedure: for assigned values of a , ℓ , m and ω , first find the angular separation constant ${}_s A_{lm}(a\omega)$ looking for zeros of the *angular* continued fraction; then replace the corresponding eigenvalue into the *radial* continued fraction, and look for its zeros as a function of ω . In principle, the convergence of the procedure for modes with large imaginary parts can be improved, as described earlier, by a wise choice of the rest, R_N , of the radial continued fraction. Expanding this rest as in formula (11) and introducing $b \equiv \sqrt{1-4a^2}$, we get for the first few coefficients: $C_0 = -1$, $C_1 = \pm\sqrt{-2i\omega b}$, $C_2 = [3/4 + i\omega(b+1) - s]$.

The angular continued fraction, considered *separately* from the radial continued fraction, is a simple and efficient tool to compute the angular eigenvalues ${}_s A_{lm}(a\omega)$ of the spin-weighted spheroidal wave equations for complex values of the argument $a\omega$. We simply start from the known Schwarzschild limit, ${}_s A_{lm}(0) = l(l+1) - s(s+1)$. Then we solve the angular continued fraction, using this value as an initial guess, to compute ${}_s A_{lm}$ for generic values of $a\omega$. In section V C we show that this simple technique yields remarkably accurate results, even for large values of $|a\omega|$.

B. Results

The most relevant feature of the Kerr quasinormal spectrum is that rotation acts very much like an external magnetic field on the energy levels of an atom, causing a *Zeeman splitting* of the quasinormal mode spectrum. We

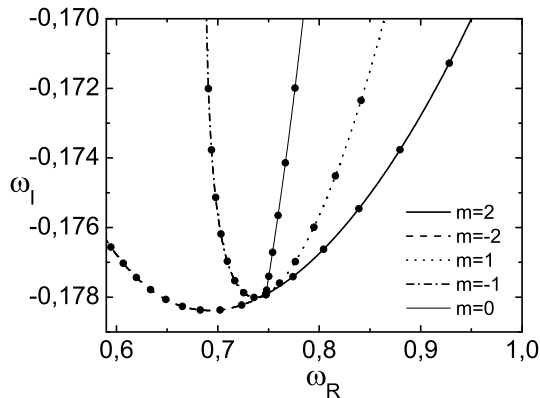


FIG. 7: “Zeeman-like” splitting of the fundamental gravitational mode with $l = 2$. We mark by dots the points corresponding to $a = 0, 0.05, 0.10, \dots, 0.5$.

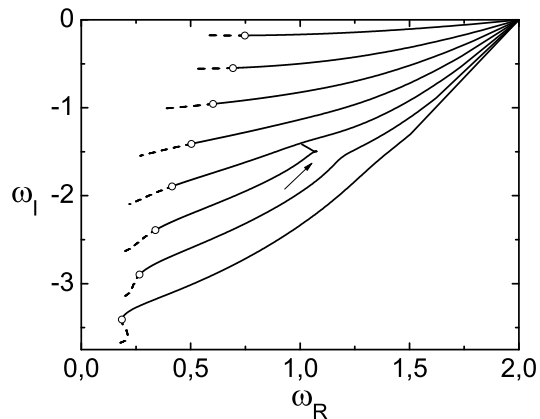


FIG. 8: Trajectory in the complex plane of the first eight Kerr quasinormal frequencies with $m = 2$ (solid lines) and $m = -2$ (dashed lines). Filled circles mark the corresponding mode in the Schwarzschild limit. An arrow indicates the small loop described by the “exceptional” quasinormal mode with $n = 6$, that does not tend to the critical frequency for superradiance (see also Figures 3 and 4 in [61]).

illustrate the splitting of the fundamental quasinormal mode in Figure 7 (see also [61]). As the rotation parameter a increases the branches with $m = 2$ and $m = -2$ move in opposite directions, being tangent to the branches with $m = 1$ and $m = -1$. In this simple case the effect of rotation on the modes is roughly proportional to m , as physical intuition would suggest. The mode with $m = 0$ has a different behavior: it “moves” very quickly along a direction in the complex plane which is roughly perpendicular to the two branches with $m \neq 0$.

In Figure 8 we show the first eight quasinormal frequencies with $m = 2$ (solid lines) and $m = -2$ (dashed lines). For large enough damping, modes with $m < 0$ are not tangent to the corresponding modes with positive m . Notice also that all modes with $n < 9$ and $m > 0$ cluster at the critical frequency for superradiance $\omega_{SR} = m\Omega$, where Ω is the angular velocity of the black hole horizon. This fact was first observed by Detweiler [62], who went on to suggest that all modes with positive m should tend to the critical frequency for superradiance as the black hole becomes extremal. It was even suggested that this could point to a marginal instability of extremal Kerr black holes. The study of the modes’ *excitation amplitudes* in the same limit led to the conclusion that such an instability does not actually occur [25, 63]. The mode with $n = 6$ (marked by an arrow) shows a peculiar deviation from the general trend, clearly illustrating the fact that some positive- m modes do *not* tend to the critical frequency for superradiance

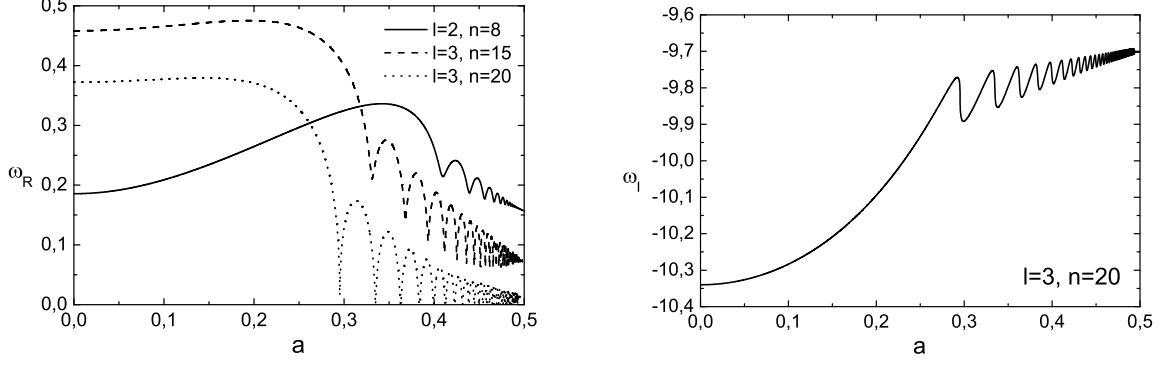


FIG. 9: Left panel: real part of Kerr modes having $m = 0$ as a function of a . Labels indicate the corresponding values of l and of the mode order n . Right panel: imaginary part of Kerr modes with $l = 3$, $m = 0$, $n = 20$ as a function of a .

in the extremal limit.

For gravitational wave emission, the dominant quasinormal mode is almost certainly the fundamental mode with $l = m = 2$. The reason is that a black hole formed in a stellar collapse or in a merger event is likely to have a rotating “bar” shape corresponding to spheroidal harmonic indices $l = m = 2$, and also that this mode is the most slowly damped, as we can see from Figure 8. Echeverria [64] found that the following analytic fit reproduces numerical data for the fundamental mode with $l = m = 2$ within about 10 %:

$$M\omega_R \simeq \left[1 - 0.63(1 - a)^{3/10}\right] \sim (0.37 + 0.19a), \quad (32)$$

$$\tau/M \sim \frac{4}{(1 - a)^{9/10}} \left[1 - 0.63(1 - a)^{3/10}\right] \sim (1.48 + 2.09a). \quad (33)$$

In these relations we restored the black hole masses; the last step is a series expansion for small values of the rotational parameter a . Fryer, Holz and Hughes produced a similar fit for the mode with $l = 2$, $m = 0$ [65].

In Figure 9 we show the real and imaginary parts of some gravitational quasinormal frequencies with $m = 0$. The looping behavior is similar to that of RN modes, and the number of loops increases with the damping of the mode. This same looping behavior was recently found by Glampedakis and Andersson for *scalar* perturbations of Kerr black holes, using a different method [38].

Figure 10 shows the trajectory in the complex plane of some scalar modes with $m = 0$. The spirals wind up very quickly as the damping grows, and the “center” of the spiral rapidly moves towards the pure-imaginary axis. In section V D we will see that the oscillation frequency of modes with $m = 0$ probably tends to *zero* as $|\omega_I| \rightarrow \infty$.

In [2] we found that for intermediate damping (say $10 \lesssim n \lesssim 50$) quasinormal frequencies belong to three different families depending on whether $m > 0$, $m = 0$ or $m < 0$. Figure 11 shows some representative results for electromagnetic modes ($s = -1$), but the qualitative behavior of gravitational and scalar modes is the same:

- 1) Modes with $m > 0$. For $10 \lesssim n \lesssim 50$, ω_R has a relative minimum as a function of a , but the numerics do not show any convergence to an asymptotic limit. Only the real part of gravitational modes with $l = m = 2$ tends to the limit $\omega_R = 2\Omega$ when $n \sim 50$ (see [1] and Figure 1 in [2]). This deceiving convergence seems related to the peculiar behavior of the angular separation constant for $|s| = l = m = 2$ (see Figure 12). For $m > 0$ most modes in the range $10 \lesssim n \lesssim 50$ approach the limiting value $\omega_R = m\Omega$ as $a \rightarrow 1/2$, but there are exceptions (see Figure 8). The imaginary parts of all modes with $m > 0$ have a separation $2\pi T_H$, where now T_H is the Hawking temperature of a Kerr black hole. The agreement with the separation of consecutive Schwarzschild quasinormal modes does not seem to be a coincidence, T_H being a non-trivial function of the rotation rate.
- 2) Modes with $m = 0$. The real and imaginary parts of these modes oscillate as a function of a , a behavior reminiscent of RN quasinormal modes. As n increases, ω_R becomes smaller. The spacing between the imaginary parts oscillates and is *not* given by $2\pi T_H$.

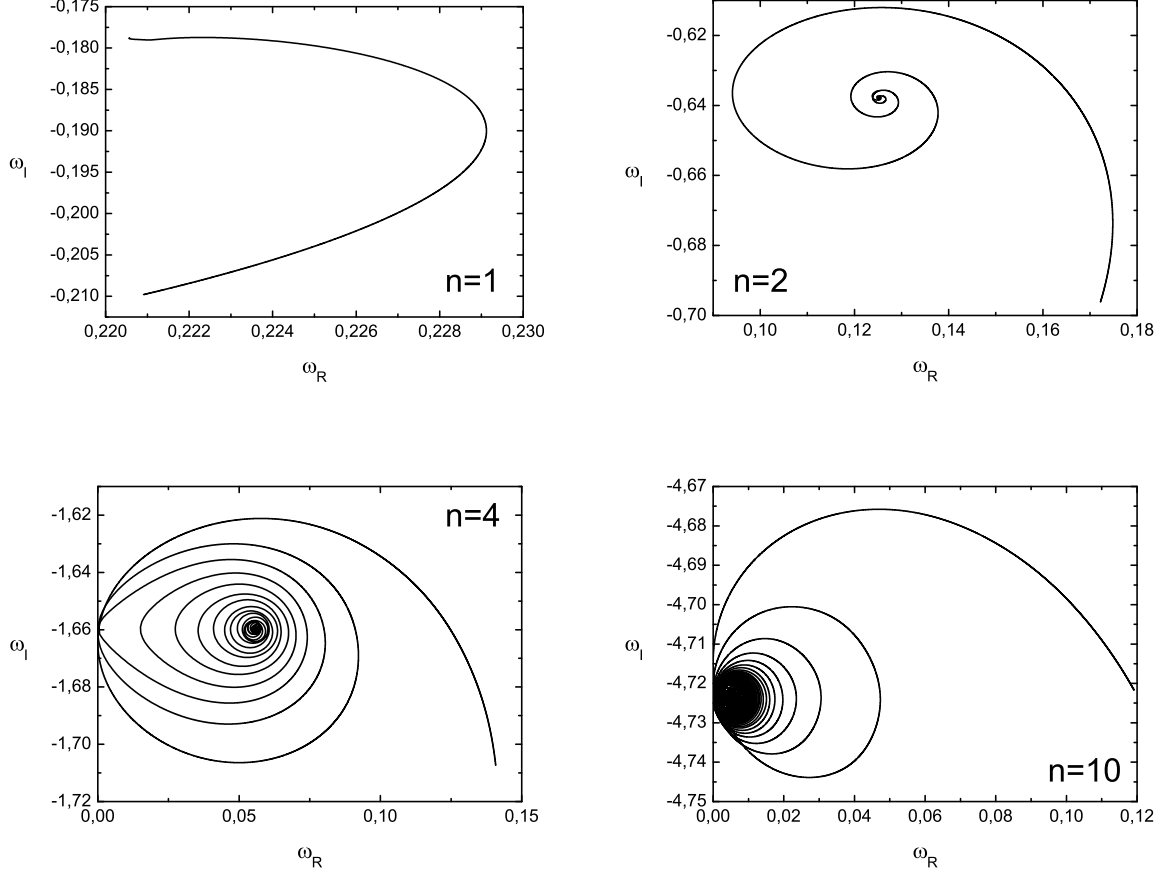


FIG. 10: Trajectories of a few scalar modes with $l = m = 0$. The different panels correspond to the fundamental mode (top left), which does not show a spiralling behavior, and to modes with overtone indices $n = 2, 4, 10$.

- 3) Modes with $m < 0$. At least for $a \gtrsim 0.25$, ω_R seems to converge to a (weakly a -dependent) limit $\omega_R \simeq m\varpi$, where $\varpi \sim 0.12$, whatever the value of l and the spin of the perturbing field. The spacing in the imaginary parts for these values of n does not show convergence, and is *not* given by $2\pi T_H$.

These results are even more puzzling than in the RN case. To probe the asymptotic regime we clearly need to push the calculation to higher damping. The main problem here is that Leaver's approach requires the *simultaneous* solution of the radial and angular continued fraction conditions. For mode order $n \gtrsim 50$ the method becomes unreliable, or it just fails to provide results. A way around this “coupling problem” is to study the asymptotic behavior of the angular equation as $|a\omega| \simeq |a\omega_I| \rightarrow \infty$. In the next section we carry out this task. We first compute numerically ${}_sA_{lm}(a\omega)$ when $\omega \simeq i\omega_I$ and $|a\omega| \rightarrow \infty$. Then we determine analytically the leading-order behavior of the separation constant. Finally, in section VD we replace this analytic expansion in the radial continued fraction, effectively getting rid of the angular equation. By this trick we can find quasinormal frequencies with $n \gg 50$ solving *only* the radial continued fraction, and ultimately determine the asymptotic behavior of $\omega_R(a)$ for Kerr black holes.

C. Angular eigenvalues

The analytical properties of the angular equation (29) and of its eigenvalues have been studied by many authors [66, 67, 68, 69, 70, 71, 72, 73]. Series expansions of ${}_sA_{lm}$ for $|a\omega| \ll 1$ have long been available, and they agree well with numerical results (see eg. [73], where some mistakes and notational differences in the previous literature are discussed and corrected).

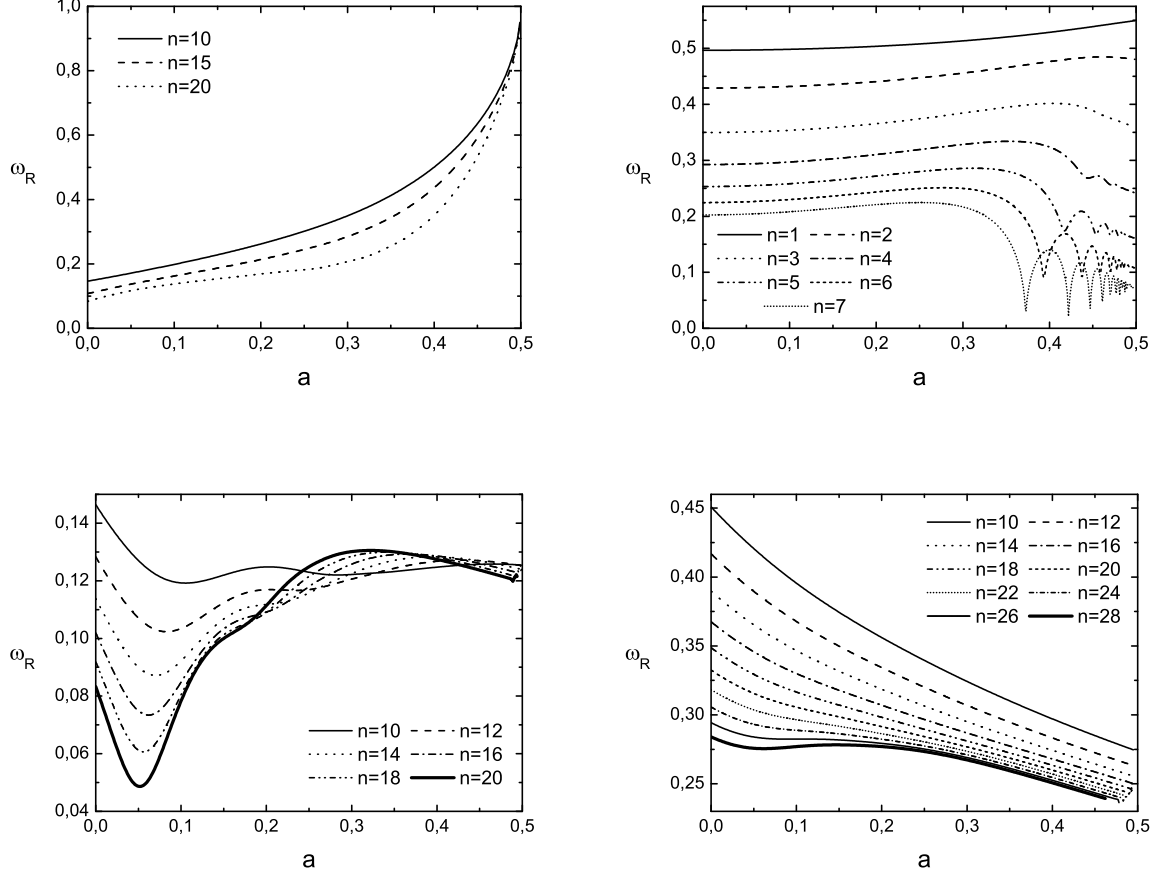


FIG. 11: Real part of electromagnetic modes with $l = m = 1$ (top left), $l = 1, m = 0$ (top right), $l = 1, m = -1$ (bottom left) and $l = 2, m = -2$ (bottom right) as a function of the rotation parameter a , for increasing values of the mode index.

Series expansions for large $|a\omega|$ have been known for a long time in the special case of $s = 0$. Such an analytical power-series expansion for large (pure real and pure imaginary) values of $a\omega$ can be found, for example, in Flammer's book [66]. Flammer's results are in good agreement with the pioneering numerical work by Oguchi [74], who computed angular eigenvalues for complex values of $a\omega$ and $s = 0$. A review of numerical methods to compute eigenvalues and eigenfunctions for $s = 0$ can be found in [67]. Recently Barrowes *et al.* studied the large frequency behavior of $s = 0$ harmonics in the complex frequency plane [68], while Falloon *et al.* developed a *Mathematica* notebook to compute $s = 0$ harmonics for general complex values of the frequency [69].

Unfortunately similar results for large values of $|a\omega|$ and general spin s are lacking. Even worse, until recently the few analytical predictions were contradictory [75]. The situation for large *real* frequencies has finally been clarified by Casals and Ottewill [76], who corrected some mistakes in reference [72]. Here we fill the remaining gap. We present numerical and analytical results for ${}_s A_{lm}$ when the frequency $a\omega$ is large and *purely imaginary*. In Flammer's language we are looking at the *prolate* case, while Casals and Ottewill deal with the *oblate* case.

We carry out our numerical calculations choosing $a\omega$ to be pure imaginary and solving Leaver's angular continued fraction as explained in section V A. Our numerical values for $s = 0$ and purely imaginary frequency (top left panel in Figure 12) are in agreement with Tables 10-12 in [66]. For complex ω and $s = 0$ we could reproduce Table 2 in [74]. As a final sanity check, we verified in a few representative cases that the *Mathematica* notebooks presented in [67, 69] are in agreement with our code when we specialize to $s = 0$.

We also verified numerically some elementary analytical properties of the eigenvalues: for example, the computed eigenvalues satisfy the relation $-{}_s A_{lm} = {}_s A_{lm} + 2s$. In the oblate case considered in [76] the eigenvalues grow quadratically, ${}_s A_{lm} \sim -|a\omega|^2$, as they should [76]. Preliminary comparisons with Casals show excellent agreement on the computed eigenvalues for all values of s [77].

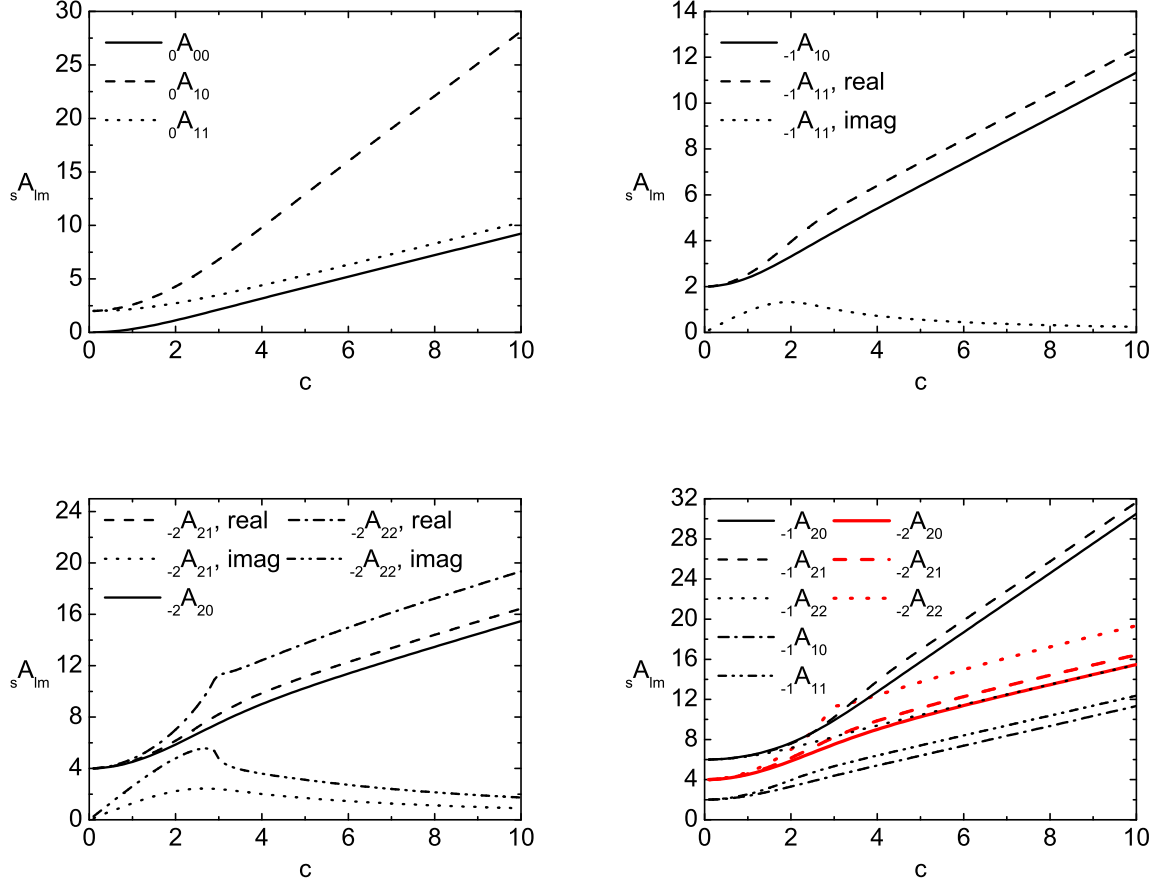


FIG. 12: Top left: angular separation constant ${}_sA_{lm}$ for $s = 0$ as a function of $c = a\omega_I$. The numerical behavior is in agreement with Flammer's asymptotic formula for the prolate case, and the separation constant is purely real. The slopes k_{lm} in ${}_sA_{lm} \sim k_{lm}c$ are either 1 or 3. Top right, bottom left: angular separation constant for $s = -1$ and $s = -2$. Now ${}_sA_{lm}$ is not purely real, but because of eq. (35) it is sufficient to compute eigenvalues with $m > 0$. In both plots, lines starting from ${}_sA_{lm} = l(l+1) - s(s+1)$ are the real parts, and lines starting from ${}_sA_{lm} = 0$ are the imaginary parts. Notice the “kink” in the real part at $c \simeq 3$ when $s = -2$ and $l = m = 2$: there is no discontinuity, just a change of slope. This peculiar behavior might explain the deceiving convergence of the quasinormal frequency to $\omega_R = 2\Omega$ that we observed in [1] for $l = m = 2$ and $s = -2$. Bottom right: real parts of ${}_sA_{lm}$ for $s = -1$ (in black) and $s = -2$ (in red). The slopes for the linear growth at large c are all consistent with Equation (38).

For $s = 0$ the series expansion given by formula (8.1.11) in [66] is an excellent approximation to the numerical data:

$$\begin{aligned} {}_0A_{lm} = & (2L+1)c - (2L^2 + 2L + 3 - 4m^2)2^{-2} - (2L+1)(L^2 + L + 3 - 8m^2)2^{-4}c^{-1} \\ & - [5(L^4 + 2L^3 + 7L + 3) - 48m^2(2L^2 + 2L + 1)]2^{-6}c^{-2} + \mathcal{O}(c^{-3}). \end{aligned} \quad (34)$$

Here we defined $c = a\omega_I$ and $L = l - |m|$. Comparison with numerical results (see the top left panel of Figure 12) shows that this expansion is reasonably accurate down to $c \simeq 2$.

For $s = -1$ and $s = -2$ the angular separation constant is complex. We can limit our calculations to positive m 's because of the following symmetry property (see eg. [40]):

$${}_sA_{l-m} = {}_sA_{lm}^*, \quad (35)$$

where the asterisk denotes complex conjugation. Numerical results for the lowest radiatable multipoles are given in Figure 12. There we plot together real and imaginary parts of the eigenvalues. It is apparent that the real part is dominant, growing linearly as $c \rightarrow \infty$.

The proportionality constant for this linear growth can be found by a straightforward generalization of Flammer's method to general values of $s \neq 0$. Define a new angular wavefunction $Z_{lm}(u)$ through [71]

$$S_{lm}(u) = (1 - u^2)^{\frac{m+s}{2}} Z_{lm}(u), \quad (36)$$

and change independent variable by defining $x = \sqrt{2c}u$, where $c^2 = -(a\omega)^2$. Substitute this in (29) to get:

$$\left[{}_sA_{lm} - \frac{cx^2}{2} - i\sqrt{2c}x - m(m+1) - \frac{2msx}{\sqrt{2c+x}} \right] Z_{lm} + (2c - x^2)Z_{lm,xx} - 2(m+s+1)xZ_{lm,x} = 0. \quad (37)$$

When $c \rightarrow \infty$, this equation becomes a parabolic cylinder function. The arguments presented in [66, 71, 72] lead to

$${}_sA_{lm} = (2L+1)c + \mathcal{O}(c^0), \quad c \rightarrow \infty, \quad (38)$$

where L is the number of zeros of the angular wavefunction inside the domain. One can show that

$$L = \begin{cases} l - |m|, & |m| \geq |s|, \\ l - |s|, & |m| < |s|. \end{cases} \quad (39)$$

Higher order corrections in the asymptotic expansion can be obtained as indicated in [66]. We will not need them in our calculation of highly damped modes.

D. High damping

To compute the asymptotic quasinormal frequencies of the Kerr black hole we use a technique similar to that described in [42]. We fix a value of the rotation parameter a . We first compute quasinormal frequencies for which $|a\omega| \sim 1$, so that formula (38) is only marginally valid. This procedure is consistent with our previous intermediate-damping calculations: for example, when we include terms up to order $|a\omega|^{-2}$ in the asymptotic expansion for ${}_0A_{lm}$ provided in [66], our new results for $a \simeq 0.1$ and $l = m = 2$ match the results for the scalar case at overtone numbers $20 \lesssim n \lesssim 30$. Then we increase the overtone index n (progressively increasing the inversion index of our “decoupled” continued fraction). Finally, we fit our numerical results by functional relations of the form:

$$\omega_R(n) = \omega_R + \omega_R^{(1)}\alpha + \omega_R^{(2)}\alpha^2 + \omega_R^{(3)}\alpha^3, \quad (40)$$

where $\alpha = 1/|\omega_I|$ or $\alpha = \sqrt{1/|\omega_I|}$. At variance with the non-rotating case [42], fits in powers of $1/|\omega_I|$ perform better, especially for small and large a . However, both fits break down as $a \rightarrow 0$: the values of higher-order fitting coefficients increase in this limit, so that subdominant terms become as important as the leading order, and the extraction of the asymptotic frequency ω_R becomes problematic. The numerical behavior of subdominant coefficients supports the expectation (which has not yet been verified analytically) that subdominant corrections are a -dependent. Therefore one has to be careful to the order in which the limits $n \rightarrow \infty$, $a \rightarrow 0$ are taken [1, 2, 28]. These observations are consistent with the fact that, in the RN case, the zero-charge limit of the asymptotic quasinormal frequency spectrum does not yield the asymptotic Schwarzschild quasinormal spectrum.

We have extracted asymptotic frequencies using two independent numerical codes. For each value of a , we found that the extrapolated value of ω_R is independent of s (Fig. 13), independent of l and proportional to m (Fig. 14):

$$\omega_R = m\varpi(a). \quad (41)$$

We obtained ω_R computing quasinormal frequencies both for scalar perturbations ($s = 0$) and for gravitational perturbations ($s = -2$). In both cases we picked $l = m = 2$. The agreement between the extrapolated behaviors of ω_R as a function of a is excellent, suggesting that both sets of results are typically reliable with an error $\lesssim 1\%$. Our results are also weakly dependent on the number of terms used in the asymptotic expansion of ${}_sA_{lm}$: this provides another powerful consistency check. We have tried to fit the resulting “universal function”, displayed in Fig. 15, by simple polynomials in the BH's Hawking temperature T and angular velocity Ω (and their inverses). None of these fits reproduces our numbers with satisfactory accuracy. It is quite likely that asymptotic quasinormal frequencies will be given by an implicit formula involving the exponential of the Kerr black hole temperature, as in the RN case [1, 28, 39].

For any a , the imaginary part ω_I grows without bound. Quite surprisingly, the spacing between modes $\delta\omega_I$ is a monotonically increasing function of a : it is not simply given by $2\pi T_H$, as some numerical and analytical calculations suggest [1, 2, 82]. A power fit in a of our numerical results yields:

$$\delta\omega_I = 1/2 + 0.0438a - 0.0356a^2. \quad (42)$$

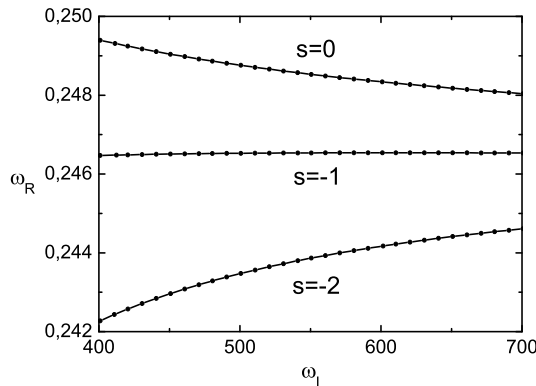


FIG. 13: Real part of high-order quasinormal frequencies for scalar ($s = 0$), electromagnetic ($s = -1$) and gravitational ($s = -2$) perturbations of a Kerr BH with $a = 0.1$ ($l = m = 2$). Quasinormal frequencies of different spins converge to the same value. For any kind of perturbation we are already deep in the region of validity of the asymptotic expansion (38), since $|a\omega| \sim 60$.

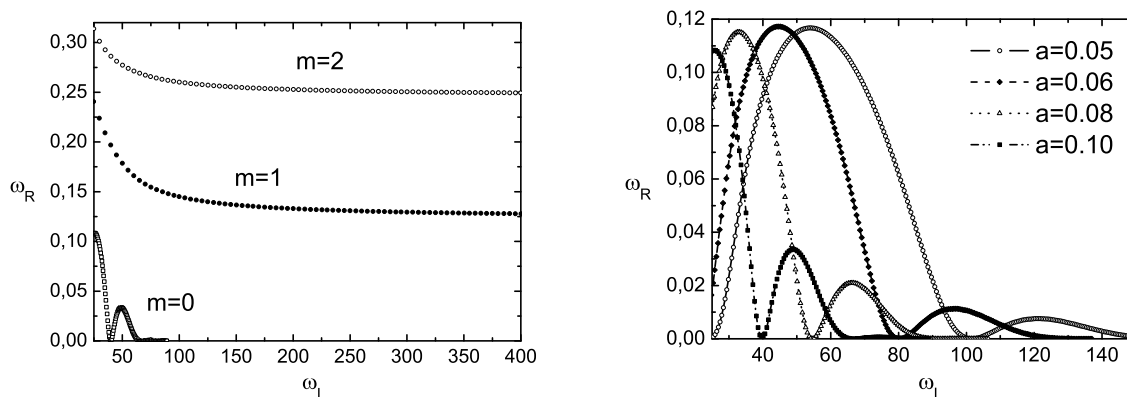


FIG. 14: Gravitational quasinormal frequencies of a Kerr BH with $a = 0.1$, $l = 2$ and different values of m . Dashed lines and open circles correspond to negative m . The asymptotic value does not depend on the sign of m , and is proportional to $|m|$. On the right we show $m = 0$ quasinormal frequencies for different values of the rotation parameter: the larger a , the faster ω_R tends to zero as $|\omega_I| \rightarrow \infty$.

VI. ALGEBRAICALLY SPECIAL MODES

Algebraically special modes of Schwarzschild black holes have been studied for a long time, but only recently their understanding has reached a satisfactory level. Among the early studies rank those of Wald [78] and of Chandrasekhar [46], who gave the exact solution of the Regge–Wheeler, Zerilli and Teukolsky equations at the algebraically special frequency. The nature of the quasinormal mode boundary conditions at the Schwarzschild algebraically special frequency is extremely subtle, and has been studied in detail by Maassen van den Brink [79].

To understand the problem, it is useful to recall that black hole oscillation modes can be classified into three groups (here we use Maassen van den Brink’s “observer-centered definition” of the boundary conditions):

- 1) “standard” quasinormal modes, which have outgoing wave boundary conditions at both sides (that is, they are outgoing at infinity and “outgoing into the horizon”);
- 2) total transmission modes from the left (TTM_L’s) are incoming from the left (the black hole horizon) and outgoing to the other side (spatial infinity);

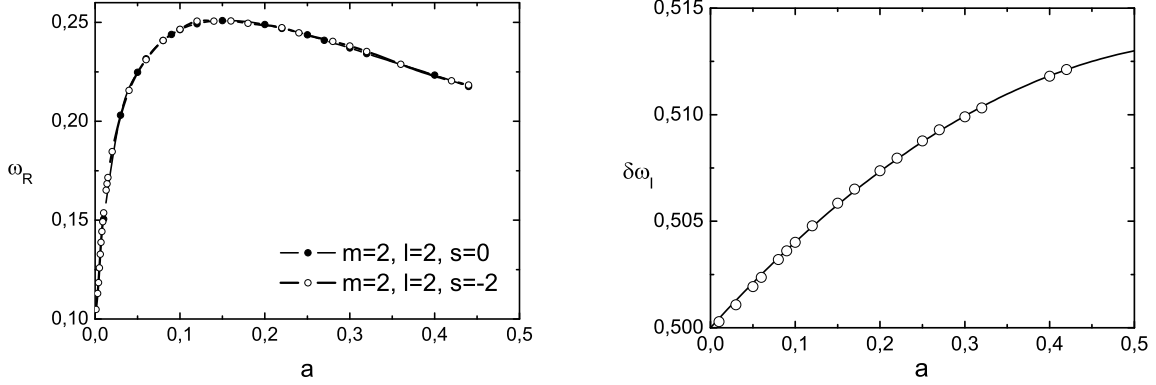


FIG. 15: Asymptotic real part $\omega_R = 2\varpi(a)$ of the $l = m = 2$ gravitational and scalar quasinormal frequencies extrapolated from numerical data: $\omega_R \rightarrow 2\varpi(1/2) \simeq 0.21$ as $a \rightarrow 1/2$. Results are independent of l , s and the sign of m .

3) total transmission modes from the right (TTM_R's) are incoming from the right and outgoing to the other side.

The Schwarzschild “algebraically special” frequency is given by formula (13) for Schwarzschild black holes [or by formula (24) for RN black holes], and traditionally it has been associated with TTM's. In fact, the algebraically special frequency is so called precisely because of the requirement that the perturbations should be “special”: they should contain only ingoing waves (the perturbed Weyl scalar $\Psi_0 \neq 0$) or only outgoing waves ($\Psi_4 \neq 0$). Speciality is equivalent to the condition that a certain quantity (the Starobinsky constant) should be zero. When Chandrasekhar determined the perturbation satisfying this condition [46] he did not check that it does indeed satisfy TTM boundary conditions. It turns out that, in general, it does not [79]. The Regge–Wheeler equation and the Zerilli equation (which are known to yield the same quasinormal mode spectrum, being related by a supersymmetry transformation) have to be treated on different footing at $\tilde{\Omega}_l$, since the supersymmetry transformation leading to the proof of isospectrality is singular there. In particular, the Regge–Wheeler equation has *no modes at all* at $\tilde{\Omega}_l$, while the Zerilli equation has *both a quasinormal mode and a TTM_L*.

Numerical calculations of algebraically special modes have yielded some puzzling results. Studying the Regge–Wheeler equation (that should have no quasinormal modes at all according to Maassen van den Brink's analysis) and not the Zerilli equation, Leaver [40] found a quasinormal mode which is very close, but not exactly located *at*, the algebraically special frequency (Table I). Namely, he found quasinormal modes at frequencies $\tilde{\Omega}'_l$ such that

$$\tilde{\Omega}'_2 = 0.000000 - 3.998000i, \quad \tilde{\Omega}'_3 = -0.000259 - 20.015653i. \quad (43)$$

Notice that the “special” quasinormal modes $\tilde{\Omega}'_l$ are such that $\Re i\tilde{\Omega}'_2 < |\tilde{\Omega}_2|$, $\Re i\tilde{\Omega}'_3 > |\tilde{\Omega}_3|$, and that the real part of $\tilde{\Omega}'_3$ is not zero. Similarly, in the extremal RN case we find a quasinormal frequency that is very close, but *not exactly equal to*, the algebraically special frequency found by Chandrasekhar. Maassen van den Brink [79] speculated that the numerical calculations may be inaccurate and that no conclusion can be drawn on the coincidence of $\tilde{\Omega}_l$ and $\tilde{\Omega}'_l$, “*if the latter does exist at all*”.

An independent calculation was carried out by Andersson [80]. Using a phase–integral method, he found that the Regge–Wheeler equation has pure imaginary TTM_R's which are very close to $\tilde{\Omega}_l$ for $2 \leq l \leq 6$. He therefore suggested that the modes he found coincide with $\tilde{\Omega}_l$, which would then be a TTM. Maassen van den Brink [79] observed again that, if all figures in the computed modes are significant, the coincidence of TTM's and quasinormal modes is not confirmed by this calculation, since $\tilde{\Omega}'_l$ and $\tilde{\Omega}_l$ are numerically (slightly) different.

Onozawa [61] showed that the Kerr mode with overtone index $n = 9$ tends to $\tilde{\Omega}_l$ as $a \rightarrow 0$, but suggested that modes approaching $\tilde{\Omega}_l$ from the left and the right may cancel each other at $a = 0$, leaving only the special (TTM) mode. He also calculated this (TTM) special mode for Kerr black holes, solving the relevant condition that the Starobinsky constant should be zero and finding the angular separation constant by a continued fraction method; his results improved upon the accuracy of those in [46].

The analytical approach adopted in [79] clarified many aspects of the problem for Schwarzschild black holes, but the situation concerning Kerr modes branching from the algebraically special Schwarzschild mode is still far from clear. In [79] Maassen van den Brink, using slow–rotation expansions of the perturbation equations, drew two basic conclusions

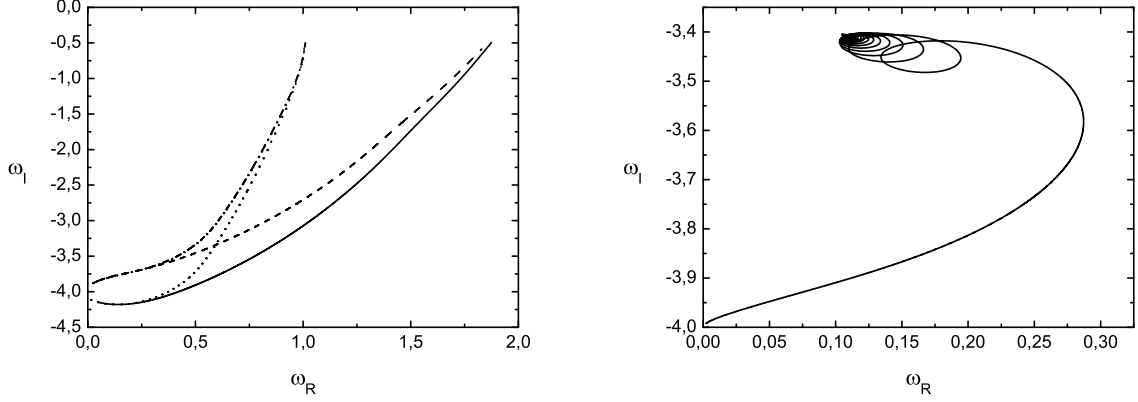


FIG. 16: The left panel shows the trajectories described in the complex- ω plane by the doublets emerging close to the Schwarzschild algebraically special frequency ($\tilde{\Omega}_2 = -4i$) when $m > 0$ and $l = 2$. Notice that the real part of modes with $m > 0$ tends to $\omega_R = m$ as $a \rightarrow 1/2$. The right panel shows the spiralling trajectory of the mode with $m = 0$.

on these modes. The first is that, for $a > 0$, the so-called Kerr special modes (that is, solutions to the condition that the Starobinsky constant should be zero [46, 61]) are all TTM's (left or right, depending on the sign of s). The TTM_R 's cannot survive as $a \rightarrow 0$, since they do not exist in the Schwarzschild limit; this is related to the limit $a \rightarrow 0$ being a very tricky one. In particular, in this limit, the special Kerr mode becomes a TTM_L for $s = -2$; furthermore, the special mode and the TTM_R cancel each other for $s = 2$. Studying the limit $a \rightarrow 0$ in detail, Maassen van den Brink reached a second conclusion: the Schwarzschild special frequency $\tilde{\Omega}_l$ should be a limit point for a multiplet of “standard” Kerr quasinormal modes, which for small a are well approximated by

$$\omega = -4i - \frac{33078176}{700009}ma + \frac{3492608}{41177}ia^2 + \mathcal{O}(ma^2) + \mathcal{O}(a^4) \quad (44)$$

when $l = 2$, and by a more complicated formula – his equation (7.33) – when $l > 2$. We numerically found quasinormal modes close to the algebraically special frequency, but they do *not* agree with this analytic prediction (not even when the rotation rate a is small).

Maassen van den Brink suggested (see note [46] in [79]) that quasinormal modes corresponding to the algebraically special frequency with $m > 0$ may have one of the following three behaviors in the Schwarzschild limit: they may merge with those having $m < 0$ at a frequency $\tilde{\Omega}'_l$ such that $|\tilde{\Omega}'_l| < |\tilde{\Omega}_l|$ (but $|\tilde{\Omega}'_l| > |\tilde{\Omega}_l|$ for $l \geq 4$) and disappear, as suggested by Onozawa [61]; they may terminate at some (finite) small a ; or, finally, they may disappear towards $\omega = -i\infty$. Recently Maassen van den Brink *et al.* [81] put forward another alternative: studying the branch cut on the imaginary axis, they found that in the Schwarzschild case a pair of “unconventional damped modes” should exist. For $l = 2$ these modes were identified by a fitting procedure to be located on the unphysical sheet lying behind the branch cut (hence the name “unconventional”) at

$$\omega_{\pm} = \mp 0.027 + (0.0033 - 4)i. \quad (45)$$

An approximate analytical calculation confirmed the presence of these modes, yielding

$$\omega_{+} \simeq -0.03248 + (0.003436 - 4)i, \quad (46)$$

in reasonable agreement with (45). If their prediction is true, an *additional* quasinormal mode multiplet should emerge near $\tilde{\Omega}_l$ as a increases. This multiplet “*may well be due to ω_{\pm} splitting (since spherical symmetry is broken) and moving through the negative imaginary axis as a is tuned*” [81]. In the following paragraph we will show that a careful numerical search indeed reveals the emergence of such multiplets, but these do not seem to behave exactly as predicted in [81].

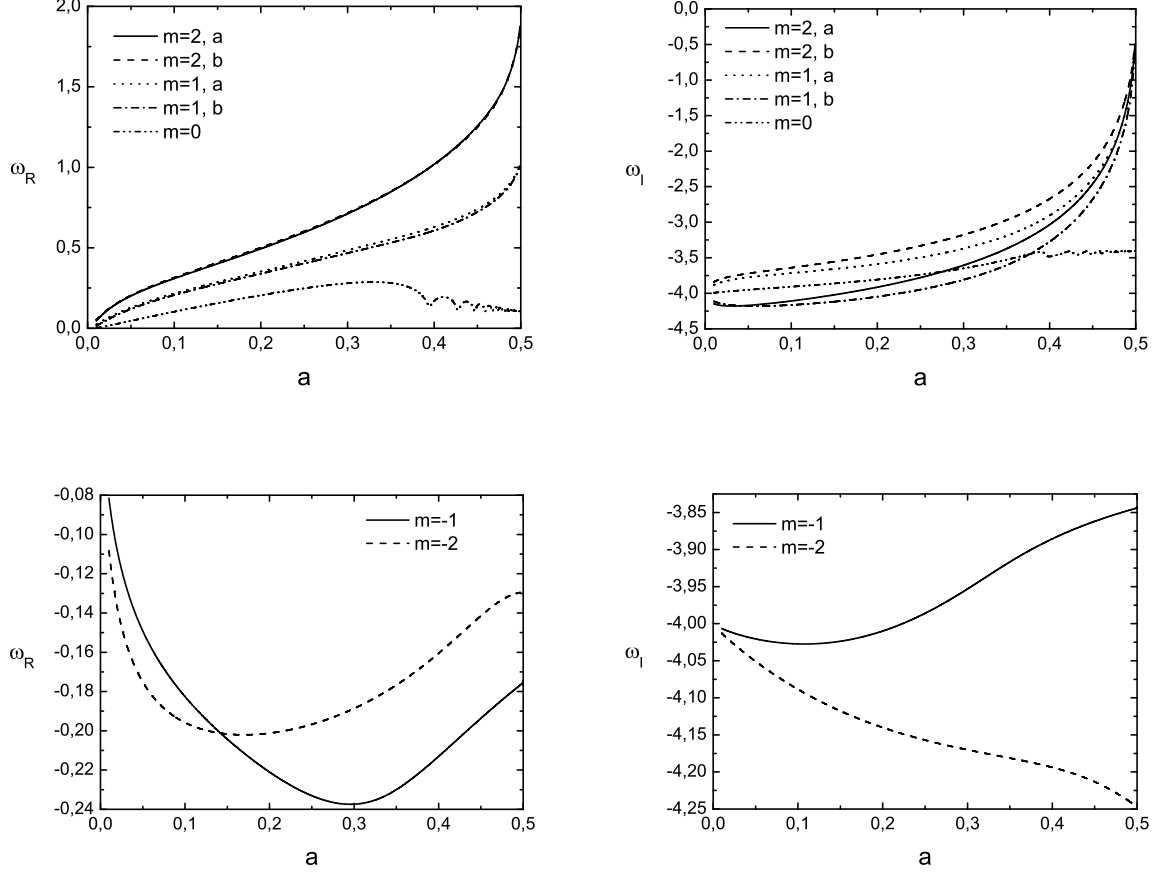


FIG. 17: The top row shows the real and imaginary parts (left and right, respectively) of the “doublet” of quasinormal modes emerging from the algebraically special frequency as functions of a . The doublets only appear when $m > 0$. We also overplot the real and imaginary parts of the mode with $l = 2$, $m = 0$ (showing the usual oscillatory behavior). The bottom row shows, for completeness, the real and imaginary parts (left and right, respectively) of modes with negative m branching from the algebraically special frequency.

A. Numerical search and quasinormal mode multiplets

As we have seen from the summary in the previous paragraph, the situation for Kerr modes branching from the algebraically special Schwarzschild mode is not clear. There are still many open questions. Is a multiplet of modes emerging from the algebraically special frequency when $a > 0$? Can quasinormal modes be matched by the analytical prediction (44) at small values of a ? If a doublet does indeed appear, as recently suggested in [81], does it tend to the algebraically special frequency $\tilde{\Omega}_2 = -4i$ as $a \rightarrow 0$, does it tend to the values predicted by formula (45), or does it tend to some other limit?

After carrying out an extensive numerical search, we have found some surprises. Our main result is shown in the left panel of Figure 16. There we show the trajectories in the complex plane of quasinormal modes with $l = 2$ and $m > 0$: a *doublet* of modes does indeed appear close to the algebraically special frequency. Both modes in the doublet tend to the usual limit ($\tilde{\Omega}_2 = m$) as $a \rightarrow 1/2$. We have tried to match these “twin” modes with the predictions of the analytical formula (44). Unfortunately, none of the two branches we find seems to agree with (44) at small a . We could only find a mode doublet for $m > 0$. For $m \leq 0$ the behavior of the modes is, in a way, more conventional. For example, in the right panel of Figure 16 we see the $l = 2$, $m = 0$ mode emerging from the standard algebraically special frequency $\tilde{\Omega}_2$ and finally describing the “usual” spirals as a increases.

In the top left panel of Figure 17 we see that the real part of the twin modes with $m \geq 0$ goes to zero as $a \rightarrow 0$ with an m -dependent slope. However, the top right panel in the same Figure shows that the imaginary part of the modes

does *not* tend to -4 as $a \rightarrow 0$. Qualitatively this behavior agrees rather well with that predicted by equation (45). Extrapolating our numerical data to the limit $a \rightarrow 0$ yields, however, slightly different numbers. Our extrapolated values for $l = 2$ are $\omega = (-4 - 0.10)i$ and $\omega = (-4 + 0.09)i$.

At present, we don't know why the doublet only appears when $m > 0$. This fact is confirmed by numerical searches close to the algebraically special frequency $\tilde{\Omega}_3$ for $l = 3$. Once again, a quasinormal mode multiplet only appears when $m > 0$. In particular, we see the appearance of a doublet similar to the modes shown in the left panel of Figure 16. Extrapolating numerical data for the $l = 3$ doublet in the limit $a \rightarrow 0$ yields $\omega = (-20 - 0.19)i$ and $\omega = (-20 + 0.24)i$.

A more careful search near the algebraically special frequency $\tilde{\Omega}_3$ surprisingly revealed the existence of other quasinormal modes. However, the additional modes we find may well be “spurious” modes due to numerical inaccuracies, since we are using the continued fraction technique in a regime ($|\omega_I| \gg 1$, $\omega_R \simeq 0$) where it is not supposed to work well.

VII. CONCLUSIONS AND OUTLOOK

The quasinormal mode spectrum of Schwarzschild, RN and Kerr black holes is overwhelmingly rich and complex. Our understanding has certainly improved over time, but many mysteries are still unsolved. The following is a (partial and necessarily biased) list of open problems.

- 1) A general lesson from the study of charged and rotating black holes seems to be: the spectrum of the limit is not the limit of the spectrum. This is a well-known fact in spectral theory, but it is quite striking in the black hole context. “Ordinary” black hole quasinormal modes suggest that there should be some continuity between the Schwarzschild and Kerr (RN) solutions as $a \rightarrow 0$ ($Q \rightarrow 0$). At a closer look, the asymptotic spectrum in the limit $|\omega_I| \rightarrow \infty$ seems to violate this continuity requirement. What is the mathematical and (more importantly) physical motivation of this discontinuity?
- 2) How does the picture change when we include *both* rotation and charge? As anticipated in the introduction, the main difficulty here is that perturbation equations for Kerr-Newman black holes are non-separable (unless we introduce some *ad hoc* approximations). Work in this direction is ongoing [84].
- 3) The algebraically special mode is a mystery on its own. Numerical methods show the presence of a quasinormal mode *close to* (but not quite *at*) the algebraically special frequencies determined by Chandrasekhar – this is true both in the Schwarzschild and in the extremal RN cases (see Figures 1 and 6). In the Kerr case, a *doublet* of modes with $m > 0$ comes out of the algebraically special Schwarzschild frequency, but no mode splitting is observed when $m \leq 0$. Analytical work on the “supersymmetry breaking” occurring at the algebraically special frequency only partially clarifies the situation [79]. We definitely need a better understanding of the meaning of quasinormal modes and total transmission modes in this situation.
- 4) The behavior of Kerr quasinormal frequencies with $m > 0$ is now better understood. Not all modes tend to the critical frequency for superradiance in the limit $a \rightarrow 1/2$. Indeed, for some modes ω_I does not even tend to zero in the extremal limit (see Figures 8 and 15). The explanation seems to be that some implicit assumptions in Detweiler's original treatment were probably overlooked [62, 83].
- 5) Our present physical understanding of highly-damped black hole oscillations is admittedly very poor. What is the meaning of the spirals we see for RN quasinormal modes (and for Kerr modes with $m = 0$)? Is the “universal” Kerr asymptotic frequency $\varpi(a)$ (Figure 15) somehow connected to other fundamental frequencies of the Kerr spacetime, eg. last stable photon orbits? Why does the RN asymptotic spectrum depend on the causally disconnected region inside the horizon? Is the same true of the Kerr spacetime? And what about Kerr-Newman black holes?

At a more fundamental level, we should go back to the original motivations behind this investigation. The complexity of the (purely classical) black hole oscillation spectrum is striking. Can we still believe that there is a link between asymptotic quasinormal frequencies and black hole quantization, or was it just a numerical coincidence? Can we really think of black holes as “quantum gravity atoms” [12, 13], being the simplest objects we can build out of gravity alone? If the analogy between classical black hole oscillations and atomic spectra holds, the bizarre nature of the quasinormal mode spectrum is telling us that there's a long way to go before we fully understand how to quantize gravity.

Acknowledgements

This short review is based on a talk given at the “Workshop on Dynamics and Thermodynamics of Black Holes and Naked Singularities” (Milan, May 2004) and on work done jointly with Vitor Cardoso, Kostas Kokkotas, Hisashi Onozawa and Shijun Yoshida. I am especially grateful to Vitor and Kostas for many comments and corrections. This work was supported in part by the National Science Foundation under grant PHY 03-53180.

-
- [1] E. Berti and K. D. Kokkotas, Phys. Rev. D **68**, 044027 (2003).
 - [2] E. Berti, V. Cardoso, K. D. Kokkotas and H. Onozawa, Phys. Rev. D **68**, 124018 (2003).
 - [3] E. Berti, V. Cardoso and S. Yoshida, Phys. Rev. D **69**, 124018 (2004).
 - [4] T. Regge, J. A. Wheeler, Phys. Rev. **108**, 1063 (1957).
 - [5] F. J. Zerilli, Phys. Rev. D **2**, 2141 (1970).
 - [6] J. A. H. Futterman, F. A. Handler, R. A. Matzner, *Scattering from black holes* (Cambridge University Press, Cambridge, England, 1988).
 - [7] S. Teukolsky, Astrophys. J. **185**, 635 (1973).
 - [8] S. Chandrasekhar, in *The Mathematical Theory of Black Holes* (Oxford University, New York, 1983).
 - [9] H.-P. Nollert, Class. Quant. Grav. **16**, R159 (1999).
 - [10] S. R. Brandt, E. Seidel, Phys. Rev. D **52**, 870 (1995).
 - [11] J. W. York, Phys. Rev. D **28**, 2929 (1983).
 - [12] S. Hod, Phys. Rev. Lett. **81**, 4293 (1998).
 - [13] J. Bekenstein, Lett. Nuovo Cim. **11**, 467 (1974); for a recent review see J. Bekenstein, in *Cosmology and Gravitation*, edited by M. Novello (Atlantisciences, France 2000), pp. 1-85; gr-qc/9808028 (1998).
 - [14] O. Dreyer, Phys. Rev. Lett. **90**, 081301 (2003).
 - [15] M. Domagala, J. Lewandowski, gr-qc/0407051.
 - [16] E. Berti, V. Cardoso and J. P. S. Lemos, gr-qc/0408099.
 - [17] K.D. Kokkotas and B.G. Schmidt, Living Rev. Relativ. **2**, 2 (1999).
 - [18] C. Vishveshwara, Nature **227**, 936 (1970).
 - [19] W. Press, Astrophys. J. **170**, L105 (1971).
 - [20] A. Nagar, G. Díaz, J. A. Pons and J. A. Font, Phys. Rev. D **69**, 124028 (2004).
 - [21] E. Pazos-Ávalos and C. Lousto, gr-qc/0409065.
 - [22] S. Chandrasekhar and S. Detweiler, Proc. R. Soc. London **A344**, 441 (1975).
 - [23] H.-P. Nollert and B. G. Schmidt, Phys. Rev. D **45**, 2617 (1992).
 - [24] N. Andersson, Proc. R. Soc. London **439**, 47 (1992).
 - [25] H. Blome and B. Mashoon, Phys. Lett. **100A**, 231 (1984); V. Ferrari and B. Mashoon, Phys. Rev. D **30**, 295 (1984).
 - [26] V. Cardoso, J. P. S. Lemos, Phys. Rev. D **67**, 084020 (2003).
 - [27] L. Motl, Adv. Theor. Math. Phys. **6** 1135 (2003).
 - [28] L. Motl and A. Neitzke, Adv. Theor. Math. Phys. **7**, 307 (2003).
 - [29] A. Neitzke, hep-th/0304080 (2003).
 - [30] B. Schutz and C. M. Will, Astrophys. J. **291**, L33 (1985).
 - [31] S. Iyer and C. M. Will, Phys. Rev. D **35**, 3621 (1987).
 - [32] S. Iyer, Phys. Rev. D **35**, 3632 (1987).
 - [33] K. Kokkotas and B. Schutz, Phys. Rev. D **37**, 3378 (1988).
 - [34] E. Seidel and S. Iyer, Phys. Rev. D **41**, 374 (1990); K. D. Kokkotas, Class. Quant. Grav. **8**, 2217 (1991).
 - [35] J. W. Guinn, C. M. Will, Y. Kojima and B. F. Schutz, Class. Quant. Grav. **7**, L47 (1990).
 - [36] N. Andersson, Proc. R. Soc. London **A439**, 47 (1992); N. Andersson and S. Linnæus, Phys. Rev. D **46**, 4179 (1992); N. Fröman, P. O. Fröman, N. Andersson and A. Hökback, Phys. Rev. D **45**, 2609 (1991); N. Andersson, M. E. Araújo and B. F. Schutz, Class. Quant. Grav. **10**, 757 (1993).
 - [37] N. Andersson, Proc. R. Soc. London **A442**, 427 (1993).
 - [38] K. Glampedakis, N. Andersson, Class. Quant. Grav. **20**, 3441 (2003).
 - [39] N. Andersson and C. J. Howls, Class. Quant. Grav. **21**, 1623 (2004).
 - [40] E. W. Leaver, Proc. Roy. Soc. Lon. **A402**, 285 (1985).
 - [41] G. Jaffé, Z. Phys. **87**, 535 (1934).
 - [42] H.-P. Nollert, Phys. Rev. D **47**, 5253 (1993). Notice that this paper uses the opposite convention on the Fourier transform with respect to Leaver’s [40], so that stable modes have positive imaginary part ω_I . One should replace $\omega \rightarrow -\omega$ in Nollert’s equations for consistency with Leaver’s conventions (that we follow here).
 - [43] E. W. Leaver, Phys. Rev. D **41**, 2986 (1990).
 - [44] H. Onozawa, T. Mishima, T. Okamura and H. Ishihara, Phys. Rev. D **53**, 7033 (1996).
 - [45] P. T. Leung, A. Maassen van den Brink, W. M. Suen, C. W. Wong and K. Young, math-ph/9909030.
 - [46] S. Chandrasekhar, Proc. R. Soc. London **A392**, 1 (1984).

- [47] S. Musiri and G. Siopsis, *Class. Quant. Grav* **20**, L285 (2003).
- [48] V. Cardoso, J. P. S. Lemos and S. Yoshida, *Phys. Rev. D* **69**, 044004 (2004).
- [49] The constant $j = 0$ for scalar and gravitational tensor perturbations, $j = 2$ for gravitational vector perturbations, $j = 2/(D - 2)$ for electromagnetic vector perturbations, $j = 2 - 2/(D - 2)$ for electromagnetic scalar perturbations.
- [50] R. A. Konoplya, *Phys. Rev. D* **68**, 024018 (2003); R. A. Konoplya, *Phys. Rev. D* **68**, 124017 (2003); E. Berti, M. Cavagliá, L. Gualtieri, *Phys. Rev. D* **69**, 124011 (2004).
- [51] V. Cardoso, J. P. S. Lemos and S. Yoshida, *JHEP* **0312**, 041 (2003).
- [52] D. Birmingham, *Phys. Lett. B* **569**, 199 (2003).
- [53] N. Andersson and H. Onozawa, *Phys. Rev. D* **54**, 7470 (1996).
- [54] Our numerical codes are in excellent agreement with the results in [53]. When comparing with their paper note, however, that Andersson and Onozawa count modes starting from $n = 0$, while we label the fundamental mode by $n = 1$, following Leaver [40].
- [55] For computational convenience, Motl and Neitzke [28] fixed units in a somewhat unconventional way. They introduced a parameter k related to the black hole charge and mass by $Q/M = 2\sqrt{k}/(1 + k)$, so that $\beta = 4\pi/(1 - k) = 1/T_H$ is the inverse black hole Hawking temperature and $\beta_I = -k^2\beta$ is the inverse Hawking temperature of the inner horizon.
- [56] S. Das, S. Shankaranarayanan, hep-th/0410209; V. Cardoso, private communication.
- [57] H. Onozawa, T. Okamura, T. Mishima and H. Ishihara, *Phys. Rev. D* **55**, 4529 (1997); T. Okamura, *Phys. Rev. D* **56**, 4927 (1997); R. Kallosh, J. Rahmfeld and W. K. Wong, *Phys. Rev. D* **57**, 1063 (1998).
- [58] S. W. Hawking, G. T. Horowitz, S. F. Ross, *Phys. Rev. D* **51**, 4302 (1995).
- [59] E. Abdalla, K. H. C. Castello-Branco, A. Lima-Santos, *Mod. Phys. Lett. A* **18**, 1435 (2003). gr-qc/0301130 (2003).
- [60] E. Berti, K. D. Kokkotas, *Phys. Rev. D* **67**, 064020 (2003).
- [61] H. Onozawa, *Phys. Rev. D* **55**, 3593 (1997).
- [62] S. Detweiler, *Astrophys. J.* **239**, 292 (1980).
- [63] K. Glampedakis, N. Andersson, *Phys. Rev. D* **64**, 104021 (2001).
- [64] F. Echeverria, *Phys. Rev. D* **40**, 3194 (1989).
- [65] C. L. Fryer, D. E. Holz, S. A. Hughes, *Astrophys. J.* **565**, 430 (2002).
- [66] C. Flammer, in *Spheroidal Wave Functions*, (Stanford University Press, Stanford, CA, 1957).
- [67] L.-W. Li, M.-S. Leong, T.-S. Yeo, P.-S. Kooi and K.-Y. Tan, *Phys. Rev. E* **58**, 6792 (1998).
- [68] B. E. Barrowes, K. O'Neill, T. M. Grzegorzczak and J. A. Kong, *Studies in Applied Mathematics* **113**, 271 (2004).
- [69] P. E. Falloon, P. C. Abbott and J. B. Wang, *Journal of Physics A* **36**, 5477 (2003). A *Mathematica* package and documentation are available at the URL <http://internal.physics.uwa.edu.au/~falloon/spheroidal/spheroidal.html>
- [70] A. A. Starobinskii and S. M. Churilov, *Sov. Phys.-JETP* **38**, 1 (1974); W. H. Press and S. A. Teukolsky, *Astrophys. J.* **185**, 649 (1973); E. D. Fackerell and R. G. Crossman, *J. Math. Phys.* **18**, 1849 (1977).
- [71] R. A. Breuer, in *Gravitational Perturbation Theory and Synchrotron Radiation*, (Lecture Notes in Physics, Vol. 44), (Springer, Berlin 1975).
- [72] R. A. Breuer, M. P. Ryan Jr. and S. Waller, *Proc. R. Soc. London* **A358**, 71 (1977).
- [73] E. Seidel, *Class. Quant. Grav.* **6**, 1057 (1989).
- [74] T. Oguchi, *Radio Science* **5**, 1207 (1970).
- [75] In [71] an attempt was made to generalize Flammer's large- $(a\omega)$ expansion for general spin s . However, the result given there for the number of zeroes of the angular wavefunction (page 115) is wrong: see [76] and Theorem 4.1 in [72]. Therefore, although the derivation is essentially correct, the expression for the leading term given in [71] is not.
- [76] M. Casals, A. C. Ottewill, gr-qc/0409012.
- [77] E. Berti, V. Cardoso and M. Casals, in preparation.
- [78] R. Wald, *J. Math. Phys. (N.Y.)* **14**, 1453 (1973).
- [79] A. Maassen van den Brink, *Phys. Rev. D* **62**, 064009 (2000).
- [80] N. Andersson, *Class. Quant. Grav.* **11**, L39 (1994).
- [81] P. T. Leung, A. Maassen van den Brink, K. W. Mak and K. Young, *Class. Quant. Grav.* **20**, L217 (2003).
- [82] A. J. M. Medved, D. Martin and M. Visser, gr-qc/0310009; T. Padmanabhan, gr-qc/0310027.
- [83] V. Cardoso, private communication.
- [84] E. Berti and K. Kokkotas, in preparation.